First induced plastid genome mutations in an alga with secondary plastids: psbA mutations in the diatom Phaeodactylum tricornutum (Bacillariophyceae) reveal consequences on the regulation of photosynthesis

Arne Materna, Sabine Sturm, Peter G. Kroth, Johann Lavaud

Journal of PHYCOLOGY
An International Journal of Algal Research

First induced plastid genome mutations in an alga with secondary plastids: psbA mutations in the diatom Phaeodactylum tricornutum (Bacillariophyceae) reveal consequences on the regulation of photosynthesis

Journal:	*Journal of Phycology*
Manuscript ID:	JPY-08-142-ART.R2
Manuscript Type:	Regular Article
Date Submitted by the Author:	n/a
Complete List of Authors:	Materna, Arne; Massachusetts Institute of Technology (MIT), Alm Laboratory, Civil and Environmental Engineering Ng Chin Yue, Sabine; University of Konstanz, Fachbereich Biologie Kroth, Peter; University of Konstanz, Fachbereich Biologie Lavaud, Johann; CNRS-University of La Rochelle, Institute for Coastal and Environmental Research
Keywords:	diatom, D1 protein, electron transport, chlorophyll fluorescence, herbicide, photosystem II, QB pocket
Category:	Physiology and Biochemistry

FIRST INDUCED PLASTID GENOME MUTATIONS IN AN ALGA WITH SECONDARY PLASTIDS: *PSBA* MUTATIONS IN THE DIATOM *PHAEODACTYLUM TRICORNUTUM* (BACILLARIOPHYCEAE) REVEAL CONSEQUENCES ON THE REGULATION OF PHOTOSYNTHESIS[1]

Arne C. Materna[†*], Sabine Sturm[†], Peter G. Kroth and Johann Lavaud[2#]

Group of Plant Ecophysiology, Biology Department, Mailbox M611, University of Konstanz, Universitätsstraße 10, 78457 Konstanz, Germany.

[†] These authors contributed equally to this work.

Journal research area: Physiology and Biochemistry

Running title: PHOTOSYNTHESIS IN *psbA* (D1) DIATOM MUTANTS

[1] Received_____ Accepted_____

[2] Author for correspondence: e-mail, johann.lavaud@univ-lr.fr

[*] Present address: Alm Laboratory, Civil and Environmental Engineering, Massachusetts Institute of Technology (MIT), 77 Massachusetts Av., 48-208, Cambridge, MA 02139USA.

[#] Present address: UMR CNRS 6250 'LIENSs', Institute for Coastal and Environmental Research, University of La Rochelle, 2 rue Olympe de Gouges, 17042 La Rochelle Cedex, France.

Abstract

Diatoms are unicellular eukaryotes playing a crucial role in the biochemistry and ecology of most aquatic ecosystems, especially because of their high photosynthetic productivity. They often have to cope with a fluctuating light climate and a punctuated exposure to excess light, which can be harmful for photosynthesis. To gain insight into the regulation of photosynthesis in diatoms, we generated and studied mutants of the diatom *Phaeodactylum tricornutum* carrying functionally altered versions of the plastidic *psbA* gene encoding the D1 protein of the photosystem II (PSII) reaction center. All analyzed mutants feature an amino acid substitution in the vicinity of the Q_B binding pocket of D1. We characterized the photosynthetic capacity of the mutants in comparison to wild-type cells, focusing on the way they regulate their photochemistry as a function of light intensity. The results show that the mutations resulted in constitutive changes of PSII electron transport rates. The extent of the impairment varies between mutants depending on the proximity of the mutation to the Q_B binding pocket and/or to the non-heme iron within the PSII reaction center. The effects of the mutations described here for *P. tricornutum* are similar to effects in cyanobacteria and green microalgae, emphasizing the conservation of the D1 protein structure among photosynthetic organisms of different evolutionary origins.

Key words: diatom, D1 protein, electron transport, chlorophyll fluorescence, herbicide, photosystem II, Q_B pocket

Abbreviations: Chl *a* and Chl *c*, chlorophyll *a* and *c*; DCMU, (3-(3, 4-diclorophenyl)-1,1-dimethylurea), LHC, light-harvesting complex; OEC, oxygen evolving complex; PAM, pulse amplitude modulation; PQ, plastoquinone; PSI and PSII, photosystem I and II; Q_A and Q_B, quinone A and B; PSII RC, PSII reaction center; WT, wild-type.

Introduction

Diatoms (Heterokontophyta, Bacillariophyceae) are a major group of microalgae ubiquitous in all marine and freshwater ecosystems. With probably more than 10.000 species, their biodiversity is among the largest of photosynthetic organisms, just after the higher plants (Mann 1999). Diatoms are assumed to contribute to about 40 % of the aquatic primary production (i.e. 20% of the annual global production), and to play a central role in the biochemical cycles of silica (which is part of their cell-wall) and nitrogen (Sarthou et al. 2005). Their productivity has contributed largely to the structure of contemporary aquatic ecosystems (Falkowski et al. 2004). In contrast to the supposed primary origin of red algae, green algae and higher plants, diatoms originate from a secondary endosymbiotic event in which a non-photosynthetic eukaryote probably engulfed a eukaryotic photosynthetic cell related to red algae and transformed it into a plastid (Keeling 2004). This peculiar evolution has led to complex cellular functions and metabolic regulations recently highlighted by the publication of the genome of two diatom species (Armbrust et al. 2004, Bowler et al. 2008), *Thalassiosira pseudonana* and *Phaeodactylum tricornutum*. It includes aspects of photosynthesis (Wilhelm et al. 2006), photoacclimation (Lavaud 2007), carbon and nitrogen metabolisms (Allen et al. 2006, Kroth et al. 2008), and response to nutrient starvation (Allen et al. 2008).

As for most microalgae, the photosynthetic efficiency and productivity of diatoms strongly depend on the underwater light climate (MacIntyre et al. 2000). Planktonic as well as benthic diatoms tend to dominate ecosystems characterised by highly turbulent water bodies (coasts and estuaries) where they have to cope with an underwater light climate with high frequency irradiance fluctuations coupled with large amplitudes.

Depending on the rate of water mixing, diatoms can be exposed to punctual or chronic excess light, possibly generating stressful conditions which impair photosynthesis (i.e. photo-inactivation/-inhibition) (Long et al. 1994, Lavaud 2007). In higher plants and cyanobacteria, the processes of PSII reaction center photo-inactivation/-inhibition are strongly influenced by the redox state of the acceptor side of photosystem II (PS II) with quinones (Q_A and Q_B) as primary electron acceptor (Vass et al. 1992, Fufezan et al. 2007).

Here we report the generation and characterization of four *psbA* mutants of *P. tricornutum*. All mutants feature distinct amino acid exchanges in the D1 protein of PSII close to or within the Q_B binding pocket. The point mutations resulted in a constitutive impairment of the PSII electron transfer in all mutants to different extents. To our knowledge this is the first report on similar mutants in an alga with secondary plastids.

Material and Methods

Strains and media used for producing the psbA *mutants of* Phaeodactylum tricornutum

Phaeodactylum tricornutum Bohlin (University of Texas Culture Collection, strain 646) was grown at 22°C under continuous illumination at 50 µmol photons m^{-2} s^{-1} in Provasoli's enriched F/2 seawater medium (Guillard and Ryther 1962) using 'Tropic Marin' artificial seawater at a final concentration of 50%, compared to natural seawater. When used, solid media contained 1.2% Bacto Agar (Difco, Sparks, USA).

Generation of psbA *mutants from* P. tricornutum

Construction of plasmid transformation vectors - Four transformation vectors were constructed harboring a 795-bp *psbA* fragment containing the Q_B binding pocket. The *psbA* inserts of each vector carried individual point mutations leading to different substitutions of the amino acid Serine encoded by the PsbA (D1) codon 264 (for details and a vector map see Supplementary Fig. S1). In addition to the non-synonymous point mutations in codon 264, a second, silent point mutation was introduced into codon 268 (TCT to TCA, nt position 804) without changing the encoded amino acid. The purpose of the second point mutation was to delete a *Bss*SI restriction site, thus allowing easy RFLP screening of putative transformants.

Biolistic transformation of P. tricornutum - Transformation of *P. tricornutum* was performed using a Bio Rad Biolistic PDS-1000/He Particle Delivery System (Bio-Rad, Hercules, USA) as described previously (Kroth, 2007). Gold Particles with a diameter of 0.1 µm served as microcarriers for the DNA constructs. Bombarded cells were allowed to recover for 24 h before being suspended in 1 mL of sterile F/2 50% medium. Transformants (250 µL) were selected at 21°C under constant illumination (35 µmol photons m^{-2} s^{-1}) on agar plates containing 5 10^{-6} M DCMU herbicide (3-(3, 4-diclorophenyl)-1,1-dimethylurea) and repeatedly streaked on fresh solid selective medium to obtain full segregation of the mutation.

Isolation of DNA and sequencing of wild-type and mutant psbA *genes*

Total nucleic acids from the WT and mutant cells were isolated via a cetyltrimethylammoniumbromide (CTAB)-based method (Doyle and Doyle 1990). Prior to the mutagenesis of *P. tricornutum* the WT *psbA* gene and the surrounding genes were

sequenced (NCBI accession no AY864816) via primer walking (GATC, Konstanz, Germany). For the molecular characterization of mutants, a 795 bp fragment of the *psbA* gene was amplified as described in Fig. S1 and both strands were fully sequenced (GATC, Konstanz, Germany).

Cell cultivation and preparation for physiological measurements

P. tricornutum WT and mutant cells were grown in 200 mL sterile F/2 50% medium (Guillard and Ryther 1962) at 21°C in airlift columns continuously flushed with sterile air. The cultures were illuminated at a light intensity of 50 µmol photons m^{-2} s^{-1} with white fluorescent tubes (OSRAM) with a 16:8 h light:dark cycle. Cells were harvested during the exponential phase of growth, centrifuged at 3000 g for 10 min and resuspended in their culture medium to a final chlorophyll (Chl) *a* concentration of 10 µg Chl *a* mL^{-1}. The algae were continuously stirred at 21°C under low continuous light. For oxygen (O_2), Chl fluorescence and thermoluminescence measurements, cells were dark-adapted 20 min prior to measurement.

Protein extraction and western-blot analysis

Cells were harvested during the exponential phase of growth as described above and subsequently grinded in liquid nitrogen. The homogenized cells were resuspended in preheated (60°C) extraction buffer (125 mM Tris/HCl (pH 6.8), 4% (w/v) SDS, 200 µM PMSF and 100 mM DTT) and after heat treatment extracted with acetone. After wash steps, the dried protein pellet was finally resuspended in extraction buffer. Total protein was separated by SDS–PAGE using 12%. Proteins were transferred electrophoretically

onto a PVDF membrane (Hybond™-P, Amersham Biosciences UK Limited, Buckinghamshire, England) and incubated with an antiserum against D1 (Anti-PsbA global antibody, AS05 084, Agrisera, Sweden). Detection was performed using the chemoluminescence detection system from Roche Diagnostics (BM Chemiluminescence Blotting Substrate POD).

Pigment extraction and analysis

Chl *a* amount was determined by spectrophotometry using the 90% acetone extraction method. For pigment extraction cells were deposited on a filter and frozen in liquid nitrogen. Pigments were extracted with a methanol:acetone (70:30, v/v) solution. Pigment analysis was performed via HPLC as previously described (Lavaud et al. 2003). Cell counts were performed using a Thoma hematocytometer.

Spectroscopy and PSI reaction center (P_{700}) concentration.

The absorption spectra were obtained at room temperature with a DW-2 Aminco (American Instrument Co., USA) spectrophotometer, half-bandwith 3 nm, speed 2 nm s^{-1}, OD = 0 at 750 nm, 50% F/2 medium as a reference. P_{700} quantity relative to Chl *a* was determined as described earlier (Lavaud et al. 2002a) with the DW-2 Aminco spectrophotometer in dual beam mode (reference at 730 nm).

Thermoluminescence

Thermoluminescence patterns were measured with a self-made thermoluminometer following the procedure previously described (Gilbert et al. 2004). Flashes were single turn-over with duration of 25 µs. Samples were adjusted to 20 µg Chl *a* mL^{-1} for measurement.

Oxygen (O_2) concentration and photosynthetic light-response (P/E) curves.

O_2 concentration was measured with a DW1-Clark electrode (Hansatech Ltd., England) at 21°C. White light of adjustable intensity (measured with a PAR-sensor, Licor inc., USA) was provided by a KL-1500 quartz iodine lamp (Schott, Mainz, Germany). Cell culture samples were dark-adapted for 20 min before measurement. P/E curves were obtained by illuminating a 2 mL sample during 5 min at various light intensities. A new sample was used for each measurement. E_K, the irradiance for saturation of photosynthetic O_2 emission was estimated from P/E curves.

Chlorophyll fluorescence induction kinetics and DCMU resistance

Chl *a* fluorescence induction kinetics were performed with two instruments: a PEA-fluorometer (Walz, Effeltrich, Germany) for short time kinetics (up to 200 ms), which allowed a classic OIJP analysis (see Fig. S4 for details), and a self-made 'continuous light' fluorometer (Parésys et al. 2005) for long time kinetics (up to 100 s). Cells were adjusted to a concentration of 5 µg Chl *a* mL^{-1} and 20 µg Chl *a* L^{-1} for the PEA- and the self-made fluorometers, respectively.

DCMU resistance was evaluated measuring the inhibition of the PSII activity *vs* increasing DCMU concentrations (see Fig. S4 for details). The kill curves with DCMU

and atrazine were performed by growing the cells on solid medium with increasing concentrations of herbicides; growth conditions were the same as described before.

Chlorophyll fluorescence yield

Chl fluorescence yield was monitored with a modified PAM-101 fluorometer (Walz, Effeltrich, Germany) as described previously (Lavaud et al. 2002a). For each experiment, 2 mL were used. Sodium bicarbonate was added at a concentration of 4 mM to prevent any limitation of the photosynthetic rate by carbon supply. When used, DCMU was incubated with the cell suspension at the beginning of the dark-adaptation period. Fluorescence parameters were defined as described in Fig. S4. 1-qP was used as a parameter to estimate the fraction of reduced Q_A (Büchel and Wilhelm 1993) where qP is the photochemical quenching of Chl fluorescence. The rate of linear electron transport was calculated as ETR = Φ PSII x PDF x α x 0.5, where Φ PSII is the PSII quantum yield for photochemistry, PDF is the irradiance, α is the PSII antenna size (equivalent to $1/I_{1/2}$ of Y_{SS}, see below).

Oxygen (O_2) yield per flash

The relative O_2 yield produced per flash during a sequence of single-turnover saturating flashes (O_2 sequence) was measured polarographically at 21°C with a flash electrode as described by Lavaud et al. 2002b. The flashes were separated by 500 ms allowing the reopening of PSII RCs by reoxidation of Q_A^-, between each flash. The procedures used to record and calculate the steady-state O_2 yiel per flash (Y_{SS}, an evaluation of the number of O_2 producing PSII RCs relative to Chl *a*), the reciprocal of

the half-saturating flash intensity of flash O_2 evolution saturation curves ($1/I_{1/2}$ of Y_{SS}, an evaluation of the PSII antenna size), and the miss probability per PSII were the ones described in Fig. S4.

Results

Generating the Phaeodactylum tricornutum psbA *mutants*

In an attempt to establish stable plastid transformation in *P. tricornutum* we aimed for allele replacement via homologous recombination. To minimize impact on the diatom we decided to substitute the wild-type (WT) *psbA* gene with slightly modified versions carrying alternative point mutations in codon 264 (Fig. S2B, green boxes). These mutations lead to single amino acid substitutions that were previously reported to induce herbicide resistance and a reduction of the electron transport within the photosystem II reaction center (PSII RC) (Ohad and Hirschberg 1992, Oettmeier 1999). Sequencing of the target region in several putative transformants revealed a variety of non-synonymous (and in some cases additional synonymous) point mutations. In all experiments the observed point mutations occurred apparently random and independently of the respective vector sequence. None of the obtained resistant strains carried the same pair of point mutations that was supposed to be introduced into *psbA* by the utilized transformation vector (data not shown). Negative control experiments involving exclusive selection without preceding transformation, and biolistic transformation without vector DNA failed to generate resistant colonies. We sequenced 1000 bp regions surrounding the Q_B pocket as well as coding and non-coding areas more distant to the *psbA* locus without finding other mutations than the ones described here. Yet, we cannot

exclude the possibility that additional mutations occurred at unknown loci. However, due to the selection on DCMU, which specifically interacts with the Q_B pocket of the D1 protein, additional mutations at other loci are likely to be detrimental and therefore selected against.

Although intriguing, this study is not focusing on the underlying molecular mechanism leading to the elevated mutation rates in the *psbA* gene; it will be the focus of a subsequent work. Instead, we characterized and compared for four selected mutants the physiological effects of different amino acid substitutions in the D1 protein of the PSII RC on the regulation of photosynthesis.

Localization of the mutations in the D1 protein and herbicide resistance of the Phaeodactylum tricornutum psbA *mutants*

The highly conserved D1 protein is part of the PSII RC in cyanobacteria and all phyla of plastid containing photosynthetic eukaryotes (Fig. S2A). The quinone B (Q_B) binding pocket is located between the DE helix and the transmembrane E helix of the D1 protein (Kern and Renger 2007). The functional relevance of the Q_B binding pocket (Fig. S2B) is highlighted by an amino acid sequence similarity of 97-98% between pennate and centric diatoms, and a similarity of ~ 90-93% between diatoms and members of the red lineage, the green lineage, and even cyanobacteria (Fig. S3). Sequencing the *psbA* genes of the four mutant strains revealed point mutations within or near the Q_B binding pocket (Fig. S2B, red squares). The mutant V219I featured an amino acid exchange (Val to Ile at position 219) in transmembrane helix D. In mutant F255I a Phe was changed to Ile in

helix DE close to the Q_B pocket. S264A carries a Ser to Ala substitution within the Q_B pocket, and in L275W, Leu was changed to Trp in the helix E.

In comparison to the wild-type (WT) the competitive binding of the herbicide DCMU to the Q_B pocket was altered to a different degree in all mutants (Fig. S4), among which S264A featured the highest resistance (3000 fold). The level of resistance was confirmed by growth curves in the presence of increasing concentrations of DCMU (not shown). S264A was also highly resistant against the herbicide atrazin (500 fold).

Photosystem and light-harvesting properties, and growth of the Phaeodactylum tricornutum psbA *mutants*

At low light intensity (50 µmol photons m^{-2} s^{-1}), the pigment contents of all the mutants and the WT cells were very similar although the mutants tended to accumulate slightly more Chl *a* per cell (see Fig. S4). The concentrations of active PSII RCs per Chl *a*, Y_{SS} and RC/CS_0, were higher in all the mutants but L275W (Fig. S4). The low concentration for L275W was confirmed via western-blot analysis (Fig. 1). The molar PSI:PSII ratio was similar in WT and mutants with the exception of L275W, for which the ratio was higher (x 1.3) ratio. The PSII LHC (light-harvesting complex) antenna size ($1/I_{1/2}$ of Y_{SS}), as well as E_K, the light intensity for saturation of photosynthesis were lower in all the mutants, with the exception of V219I (Fig. S4).

We compared the physiological effects of the four mutations by measuring thermoluminescence, flash oxygen (O_2) yield emission (O_2 sequence) and Chl *a* fluorescence induction kinetics. WT cells showed the expected thermoluminescence pattern with a strong B band (Fig. 2A) (Eisenstadt et al. 2008). While V219I showed the

same pattern, in F255I and S264A the temperature of the maximal signal was shifted from 22°C to about 7°C and had significantly lowered amplitude (Fig. 2A). The O_2 sequences were highly damped in dark-adapted cells of F255I, S264A and L275W (Fig. 2B) due to an increase in the miss probability (Fig. S4). In addition, in S264A and to a lesser extent in F255I (not shown), the O_2 production was increased at flash n°2 (due to an increase of 10-20% of the S_1 dark state in S264A compared to the WT) while in L275W, the maximum was at the flash n°4 instead of n°3. Chl *a* fluorescence induction kinetics are shown in Fig. 2C and Fig. 2D. All the mutants showed higher J ($Q_AQ_B^-/Q_A^-Q_B^-$ state) and lower I ($Q_A^-Q_B^{2-}$ state) phases (Fig. 2C and Fig. S4) reflecting an impairment of the Q_A-Q_B electron transfer. The phenotype of V219I was the closest to WT phenotype while F255I and L275W showed a significantly higher J phase (+ 23 and 57%, respectively). S264A showed a drastically increased (by 71%) and delayed J phase and, in contrast to the other mutants, an increased I phase (see inset Fig. 2C and Fig. S4). When recorded over a longer time scale (100 s) and at continuous illumination, the pattern of the fluorescence induction kinetics of S264A and L275W was different (only L275W is shown, Fig. 2D). In S264A and L275W, the amplitude of the I-45 ms peak increased and the whole pattern of the kinetics was disturbed.

The F_0 Chl *a* fluorescence level was increased in all mutants (Fig. S4). Adding DCMU (resulting in inhibition of electron transport between Q_A and Q_B) to WT cells resulted in an increased F_0 (195 ± 6.5) comparable to S264A and L275W. When grown at low light intensity (50 µmol photons m^{-2} s^{-1}) all mutants showed a maximum photosynthetic efficiency of PSII (F_v/F_m, Fig. S4) which was similar to the WT cells, except for L275W (- 19%). When measured at an equivalent irradiance, the effective PSII quantum

yield (Φ PSII, Fig. S4) was the same for WT cells and V219I, but lower in the other mutants. These values were in accordance with the steady-state electron transport rate per PSII (ET_0/CS_0, Fig. S4). Addition of DCMU to the WT resulted in a decreased Φ PSII (0.38), similar to that of S264A and L275W.

Only L275W showed a reduced (- 26%) growth rate (μ, Fig. S4) and final maximal biomass (Fig. S5). Although F255I and S264A reached the same final biomass with the same growth rate as the WT, they showed a 24 h delay (see days 3 and 2, respectively, Fig. S5).

Photosynthetic capacity of the Phaeodactylum tricornutum psbA *mutants as a function of the light intensity*

The light intensity dependent impairment of the Q_A-Q_B electron transfer was evaluated by measuring 1-qP, a fluorescence parameter which estimates the fraction of reduced Q_A (Büchel and Wilhelm 1993). While 1-qP was similar in WT and in V219I, it was highest in S264A and L275W (Fig. 3A). The difference in the extent of Q_A reduction was also found at rather low light intensities (inset Fig. 3A) as indicated by the ratios of the extent of the I-45 ms peak from the long-time fluorescence induction kinetics of mutant versus WT (see Fig. 2D). In S264A and L275W, 1-qP reached saturation earlier (between 250 and 400 μmol photons m^{-2} s^{-1}) than in WT cells. In F255I, the extent of Q_A reduction was higher than in WT up to a light intensity of 400 μmol photons m^{-2} s^{-1}. The direct consequences of the impaired Q_A-Q_B electron transfer were changed amplitudes of the electron transport rate per PSII (ETR) as well as altered patterns of ETR as a function of light intensity (Fig. 3B). The maximum ETR was decreased in all the mutants but to a

different extent, thus confirming the values for ET_0/CS_0 (Fig. S4). In contrast to WT and the other mutants, ETR was already maximal in S264A and L275W at a light intensity of 250 µmol photons m^{-2} s^{-1}; at this light intensity the extent of Q_A reduction was close to its maximum (Fig. 3A).

Discussion

Three out of the four *psbA* mutants showed a phenotype clearly distinct from the WT (see Fig. 4). Obviously, the observed amino acid substitutions hold implications for the phenotype of the mutants. The phenotypic effects described in this study allow various insights into the functionality of mutated residues or domains within the D1 protein.

A mutation which slightly affects the photosynthetic efficiency: V219I

In response to the slightly increased reduction state of Q_A (+ 10%) and the decreased (about 5%) ETR per PSII, in V219I the number of PSII RCs was increased (14 to 22%, depending on the method) to maintain a photosynthetic activity similar to the WT as reflected also by its growth pattern. Hence, the exchange of Val to Ile at the position 219 in the helix D appears to be too distant from the Q_B binding pocket to significantly disturb the electron transport within the PSII RC in *P. tricornutum*.

Effects of mutations within the Q_B binding pocket: F255I and S264A

The residues Phe_{255} and Ser_{264} bind the head group of Q_B (Kern and Renger 2007). The electron transport between Q_A and Q_B in F255I was significantly impaired (Fig. 4)

slowing down the reoxidation of Q_A^- as illustrated by the increased $Q_AQ_B^-/Q_A^-Q_B^-$ state. It was especially visible with the pattern of thermoluminescence which resembles the one reported in *P. tricornutum* for WT cells treated with DCMU (abolishment of the B band and increase of the Q band) (Eisenstadt et al. 2008). Backward electron transfer from Q_B^- to Q_A, as illustrated by an enhanced F_0 in photochemically inactive PSII RCs (Xiong et al. 1997), might partially explain the increased concentration of Q_A^-. As a consequence, the miss probability of the S state-cycle was increased, the S_1 state was stabilized (Perewoska et al. 1994) and the lifetimes of the redox states S_2 and S_3 increased (Gleiter et al. 1992), indicating a disturbed OEC operation. In order to compensate the decreased photochemistry of PSII, in F255I the number of PSII RCs increased (Fig. 4), reflected by a slight increase of Chl *a* per cell as also reported for higher plants (Srivasatava et al. 1994). Nevertheless, the overall amount of pigments per Chl *a* did not change, thus the antenna size per PSII decreased leading to a similar increase in E_K. Decreasing the PSII antenna size is known to be a straightforward way to relief from high excitation pressure on PSII due to a slowed down electron flow within the PSII RC because of mutations, herbicides, environmental stress, or other factors. Similarly, Wagner et al. (2006) suggested that in *P. tricornutum* an increased number of photosynthetic units together with decreased size of these units might allow maximization of photochemistry at different light regimes which might be the case in mutants F255I and S264A. In spite of all these changes, the potential for photochemistry, qP, was decreased at intermediary irradiances (up to 400 µmol photons m^{-2} s^{-1}). At high light intensities, the ETR was reduced (Fig. 4) reflecting the decrease of the PSII antenna size and of Φ PSII.

S264A showed a more drastic reaction compared to F255I regarding the Q_A^- reoxidation, the electron back transfer Q_B^- to Q_A, but also the Q_B^-/Q_B^{2-} reoxidation (increased $Q_A^-Q_B^{2-}$ state) (Fig. 4). Consequently, the operation of the OEC S-state cycle was strongly disturbed similar to the pattern of the fluorescence induction kinetics, illustrating the consequence of the modified Q_A-Q_B redox state on the whole electron transport chain and especially on the redox state of the plastoquinone (PQ) pool (Lazar 2006, Papageorgiou et al. 2007). As F255I, S264A reacted by increasing the PSII number. qP was largely diminished which usually reflects accumulation of dysfunctional, highly reduced PSII RCs. It led to a decrease in ETR at all light intensities. Both qP and ETR were saturated at a much lower irradiance than the WT. The exchange of Ser to Ala probably modified the spatial arrangement of the Q_B pocket (Gleiter et al. 1992, Perewoska et al. 1994), as illustrated by the high DCMU resistance, and greatly impaired not only the redox state of Q_B but the binding of Q_B itself (Della Chiesa et al. 1997).

Effects of a mutation close to the non-heme iron binding site: L275W

Leu_{275} is close to one of the Histidines binding the non-heme iron atom (His_{272} in helix E, grey bar in Fig. S2), as well as at nearly equal distance between Q_A and Q_B (Kern and Renger 2007). The effect of the L275W mutation on the photosynthetic ability per PSII was similar to the point mutation S264A (Fig. 4) but showed a much disturbed OEC operation and a reduction of Q_A which was already high (1.2-1.3 times the WT values) at lower light intensities than used for growing cells. Ultimately, L275W showed a decreased growth rate under low light as well as the inability to reach the same final maximal biomass. The main difference compared to the other mutants was the reduced

amount of active PSII (Fig. 4), demonstrated by a disturbed D1 repair cycle. Mutations close to or within the Q_B pocket have been reported to modify the D1 turnover either by accelerating its damage and/or by inhibiting its proteolysis and/or synthesis (Della Chiesa et al. 1997, Nishiyama et al. 2006). Thus, it is very likely that in L275W there is a mixed population of active and inactive PSII, even at low light intensities (Mohanty et al. 2007), which is supported by the high F_0 level and the lowest F_v/F_m. In contrast to the other mutants, L275W responded to the point mutation by modifying the architecture of the photosynthetic apparatus as illustrated by the increase of the PSI:PSII stochiometry (Fig. 4). This attempt to maintain a reasonable photosynthetic activity might lead to an increased capacity for PSI cyclic electron flow as in higher plants that show a deficient linear electron transport (Kotakis et al. 2006).

In a series of papers (reviewed in van Rensen et al. 1999), Govindjee and co-workers showed that the exchange of the residue Leu_{275} significantly perturbs the Q_A-Fe-Q_B structure, the protonation of Q_B^{2-} (Xiong et al. 1997) and subsequently the PQ redox state. It is thus likely that the phenotype of L275W is due to the close vicinity of the point mutation to both the Q_B pocket and the non-heme iron atom binding sites which functionally affects the properties of both the Q_A and Q_B pockets (Vermaas et al. 1994).

Effects of similar mutations in cyanobacteria and green algae

The effects of the mutations described here for the diatom *P. tricornutum* are similar to effects of the same mutations reported in other photosynthetic organisms. For example, it has also been concluded that in *Chlamydomonas reinhardtii* (Erickson et al. 1989) the V219I amino acid substitution does not significantly disturb the electron

transport within the PSII RC. Also, the effects of the F255I, S264A and L275W mutations have been described in cyanobacteria (*Synechocystis* and *Synechococcus*) and *C. reinhardtii* (Erickson et al. 1989, Etienne 1990, Gleiter et al. 1992, Kless et al. 1994, Perewoska et al. 1994). Remarkably, the S264A induced DCMU resistance was much higher in *P. tricornutum* than in all previously studied organisms (Gleiter et al. 1992).

Conclusion

Our results illustrate that not only the substitution loci but also the nature of the exchanged amino acids are essential in modifying the spatial arrangement and properties of the D1 protein (Kless and Vermaas 1994). Ultimately, such structural changes, especially in the Q_B binding pocket, are defining the electron transport rate within the PSII RC (Lardans et al. 1998, Oettmeier 1999). The fact that photosynthesis is impaired at different levels in the *P. tricornutum psbA* mutants described here (see Fig. 4) provides a unique opportunity to further study the regulation of photosynthesis in diatoms.

Acknowledgements

This work was supported by the European network MarGenes (QLRT-2001-01226 to PGK), the University of Konstanz (University of Konstanz, 'Anreizsystem zur Frauenförderung' to SS and JL) and the DFG (grant LA2368/2-1 to JL). We thank I. Adamska (University of Konstanz), C. Bowler (ENS Paris) and C. Wilhelm (University of Leipzig) for the access to some of the instruments used here and for helpful discussions, D. Ballert for technical assistance, V. Reiser and P. Huesgen (University of Konstanz), B. Rousseau (ENS Paris), T. Jakob and H. Wagner (University of Leipzig) for

435 the help with some of the experiments. This work is part of the PhD project of ACM and
436 of the Diploma work of SS.
437
438 **References**
439 Allen, A. E., Vardi, A. & Bowler, C. 2006. An ecological and evolutionary context for
440 integrated nitrogen metabolism and related signaling pathways in marine diatoms. *Curr.*
441 *Opin. Plant Biol.* 9:264-73
442 Allen, A. E., LaRoche, J., Maheswari, U., Lommer, M., Schauer, N., Lopez, P. J.,
443 Finazzi, G., Fernie, A. R. & Bowler, C. 2008. Whole-cell response of the pennate diatom
444 *Phaeodactylum tricornutum* to iron starvation. *Proc. Natl. Acad. Sci. USA* 105:10438-
445 10443
446 Armbrust, E. V., Berges, J. A., Bowler, C., Green, B. R., Martinez, D., Putnam, N. H.,
447 Zhou S., Allen, A. E., Apt, K. E., Bechner, M., Brzezinski, M. A., Chaal, B. K., Chiovitti,
448 A., Davis, A. K., Demarest, M. S., Detter, J. C., Glavina, T., Goodstein, D., Hadi, M. Z.,
449 Hellsten, U., Hildebrand, M., Jenkins, B. D., Jurka, J., Kapitonov, V. V., Kröger, N., Lau,
450 W. W. Y., Lane, T. W., Larimer, F. W., Lippmeier, J. C., Lucas, S., Medina, M.,
451 Montsant, A., Obornik, M., Parker, M. S., Palenik, B., Pazour, G. J., Richardson, P. M.,
452 Rynearson, T. A., Saito, M. A., Schwartz, D. C., Thamatrakoln, K., Valentin, K., Vardi,
453 A., Wilkerson, F. P. & Rokhsar, D. S. 2004. The genome of the diatom *Thalassiosira*
454 *pseudonana*: Ecology, evolution and metabolism. *Science* 306:79-86
455 Bowler, C., Allen, A. E., Badger, J. H., Grimwood, J., Jabbari, K., Kuo, A., Maheswari,
456 U., Martens, C., Maumus, F., Otillar, R. P., Rayko, E., Salamov, A., Vandepoele, K.,
457 Beszteri, B., Gruber, A., Heijde, M., Katinka, M., Mock T., Valentin, K., Vérret, F.,

Berges, J.A,. Brownlee, C., Cadoret, J.P., Chiovitti, A., Choi, C.J., Coesel, S., De Martino, A., Detter, J. D., Durkin, C., Falciatore, A., Fournet, J., Haruta, M., Huysman, M., Jenkins, B. D., Jiroutova, K., Jorgensen, R. E., Joubert, Y., Kaplan, A., Kroeger, N., Kroth, P. G., La Roche, J., Lindquist, E., Lommer, M., Martin-Jézéquel, V., Lopez, P. J., Lucas, S., Mangogna, M., McGinnis, K., Medlin, L. K., Montsant, A., Oudot-Le Secq, M. P., Napoli, N., Obornik, M., Petit, J. L., Porcel, B. L., Poulsen, N., Robison, M., Rychlewski, L., Rynearson, T. A., Schmutz, J., Schnitzler Parker, M., Shapiro, H., Siaut, M., Stanley, M., Sussman, M. R., Taylor, A., Vardi, A., von Dassow, P., Vyverman, W., Willis, A., Wyrwicz, L. S., Rokhsar, D.S., Weissenbach, J., Armbrust, E. V., Green, B. R., Van de Peer, Y., Grigoriev, I. V. (2008) The *Phaeodactylum* genome reveals the evolutionary history of diatom genomes. Nature 455: online, doi:10.1038/nature07410.

Büchel, C. & Wilhelm, C. 1993. *In vivo* analysis of slow chlorophyll fluorescence induction kinetics in algae: progress, problems and perspectives. *Photochem. Photobiol.* 58:137-48

Della Chiesa, M., Friso, G., Deak, Z., Vass, I., Barber, J. & Nixon, P. 1997. Reduced turnover of the D1 polypeptide and photoactivation of electron transfer in novel herbicide resistant mutants of *Synechocystis* sp. PCC 6803. *Eur. J. Biochem.* 248:731-40

Doyle, J. J. & Doyle, J. L. 1990. A rapid total DNA preparation procedure for fresh plant tissue. *Focus* 12:13-5

Eisenstadt, D., Ohad, I., Keren, I. & Kaplan, A. 2008. Changes in the photosynthetic reaction center II in the diatom *Phaeodactylum tricornutum* result in non-photochemical fluorescence quenching. Environ. Microbiol. 10:1997-2007

480 Erickson, J. M., Pfister, K., Rahire, M., Togasaki, R. K., Mets, L. & Rochaix, J.-D. 1989.
481 Molecular and biophysical analysis of herbicide-resistant mutants of *Chlamydomonas*
482 *reinhardtii*: Structure-function relationship of the photosystem II D1 polypeptide. *Plant*
483 *Cell* 1:361-71
484 Etienne, A.-L., Ducruet, J.-M., Ajlani, G. & Vernotte, C. 1990. Comparative studies on
485 electron transfer in photosystem II of herbicide-resistant mutants from different
486 organisms. *Biochim. Biophys. Acta* 1015:435-40
487 Falkowski, P. G., Katz, M. E., Knoll, A. H., Quigg, A., Raven, J. A., Schofield, O. &
488 Taylor, F. R. J. 2004. The evolution of modern phytoplankton. *Science* 305:354-60
489 Fufezan, C., Gross, C. M., Sjödin, M., Rutherford, A. W., Krieger-Liszkay, A. &
490 Kirilovsky, D. 2007. Influence of the redox potential of the primary quinone electron
491 acceptor on photoinhibition in photosystem II. *J. Biol. Chem.* 282:12492-502
492 Gilbert, M., Wagner, H., Weingart, I., Nieber, K., Tauer, G., Bergmann, F., Fischer, H. &
493 Wilhelm, C. 2004. A new type of thermoluminometer:A highly sensitive tool in applied
494 photosynthesis research and plant stress physiology. *J. Plant Physiol.* 161:641-51
495 Gleiter, H. M., Ohad, N., Kolke, H., Hirschberg, J., Renger, G. & Inoue, Y. 1992.
496 Thermoluminescence and flash-induced oxygen yield in herbicide resistant mutants of the
497 D1 protein in *Synechococcus* PCC7942. *Biochim. Biophys. Acta* 1140:135-43
498 Guillard, R. R. R. & Ryther, J. H. 1962. Studies of marin planktonic diatoms. 1. *C. nana*
499 (Hustedt) and *D. confervacea* (Cleve). *Gran. Can. J. Microbiol.* 8:229-38
500 Ishikawa, Y., Nakatani, E., Henmi, T., Ferjani, A., Harada, Y., Tamura, N. & Yamamoto,
501 Y. 1999. Turnover of the aggregates and cross-linked products of the D1 protein

generated by acceptor-side photoinhibition of photosystem II. *Biochim. Biophys. Acta* 1413:147-58

Keeling, P. 2004. A brief history of plastids and their hosts. *Protist* 155:3-7

Kern, J. & Renger, G. 2007. Photosystem II: Structure and mechanism of the water:plastoquinone oxidoreductase. *Photosynth. Res.* 94:183-202

Kless, H., Oren-Shamir, M., Malkin, S., McIntosh, L. & Edelman, M. 1994. The *D-E* region of the D1 protein is involved in multiple quinone and herbicide interactions in photosystem II. *Biochemistry* 33:10501-07

Kless, H. & Vermaas, W. 1994. Many combinations of amino acid sequences in a conserved region of the D1 protein satisfy photosystem II function. *J. Mol. Biol.* 246:120-31

Kotakis, C., Petropoulou, Y., Stamatakis, K., Yiotis, C. & Manetas, Y. 2006. Evidence for active cyclic electron flow in twig chlorenchyma in the presence of an extremely deficient linear electron transport activity. *Planta* 225:245-53

Kroth, P. G. 2007. Genetic transformation - a tool to study protein targeting in diatoms. *In* Van der Giezen, M. ed *Methods in Molecular Biology - Protein Targeting Protocols*. Humana Press, Totowa, USA, pp. 257-68

Kroth, P. G., Chiovitti, A., Gruber, A., Martin-Jézéquel, V., Mock, T., Schnitzler Parker, M., Stanley, M. S., Kaplan, A., Caron, L., Weber, T., Maheswari, U., Armbrust, V. E. & Bowler, C. 2008. A model for carbohydrate metabolism in the diatom *Phaeodactylum tricornutum* deduced from comparative whole genome analysis. *PLoS One* 3:e1426.

Lardans, A., Förster, B., Prasil, O., Falkowski, P. G., Sobolev, V., Edelman, M., Osmond, C. B., Gillham, N. W. & Boynton, J. E. 1998. Biophysical, biochemical, and

physiological characterization of *Chlamydomonas reinhardtii* mutants with amino acid substitutions at the Ala^{251} residue in the D1 protein that result in varying levels of photosynthetic competence. *J. Biol. Chem.* 273:11062-91

Lavaud, J. 2007. Fast regulation of photosynthesis in diatoms: mechanisms, evolution and ecophysiology (a review). *Funct. Plant Sci. Biotech.* 1:267-87

Lavaud, J. & Kroth, P. 2006. In diatoms, the transthylakoid proton gradient regulates the photoprotective non-photochemical fluorescence quenching beyond its control on the xanthophyll cycle. *Plant Cell Physiol.* 47:1010-6

Lavaud, J., Rousseau, B. & Etienne, A.-L. 2003. Enrichment of the light-harvesting complex in diadinoxanthin and implications for the nonphotochemical quenching fluorescence quenching in diatoms. *Biochemistry USA* 42:5802-8

Lavaud, J, van Gorkom, H. & Etienne, A.-L. 2002b. Photosystem II electron transfer cycle and chlororespiration in planktonic diatoms. *Photosynth. Res.* 74:51-9

Lavaud, J., Rousseau, B., van Gorkom, H. & Etienne, A.-L. 2002a. Influence in the diadinoxanthin pool size on photoprotection in the marine planktonic diatom *Phaeodactylum tricornutum*. *Plant Physiol.* 129:1398-406

Lazar, D. 2006. The polyphasic chlorophyll *a* fluorescence rise measured under high intensity of exciting light. *Funct. Plant Biol.* 33:9-30

Long, S., Humphries, S. & Falkowski, P. 1994. Photoinhibition of photosynthesis in nature. *Ann. Rev. Plant Physiol. Plant Mol. Biol.* 45:633-62

MacIntyre, H. L., Kana, T. M. & Geider, R. J. 2000. The effect of water motion on short-term rates of photosynthesis by marine phytoplankton. *TRENDS Plant Sci.* 5:12-7

Mann, D. G. 1999. The species concept in diatoms. *Phycologia* 38:437-495

548 Mohanty, P., Allakhverdiev, S. I. & Murata, N. 2007. Application of low temperatures
549 during photoinhibition allows characterization of individual steps in photodamage and the
550 repair of photosystem II. *Photosynth. Res.* 94:217-24
551 Nishiyama, Y., Allakhverdiev, S. I. & Murata, N. 2006. A new paradigm for the action of
552 reactive oxygen species in the photoinhibition of photosystem II. *Biochim. Biophys. Acta*
553 1757:742-9
554 Oettmeier, W. 1999. Herbicide resistance and supersensitivity in photosystem II. *Cell.*
555 *Mol. Life Sci.* 55:1255-77
556 Ohad, N. & Hirshberg, J. 1992. Mutations in the D1 subunit of photosystem II distinguish
557 between quinone and herbicide binding sites. *Plant Cell* 4:273-82
558 Papageorgiou, G. C., Tsimilli-Michael, M. & Stamatakis, K. 2007. The fast and slow
559 kinetics of chlorophyll *a* fluorescence induction in plants, algae and cyanobacteria: a
560 viewpoint. *Photosynth. Res.* 94:275-90
561 Parésys, G., Rigart, C., Rousseau, B., Wong, A. W. M., Fan, F., Barbier, J.-P. & Lavaud,
562 J. 2005. Quantitative and qualitative evaluation of phytoplankton populations by
563 trichromatic chlorophyll fluorescence excitation with special focus on cyanobacteria.
564 *Water Res.* 39:911-21
565 Perewoska, I., Etienne, A.-L., Miranda, T. & Kirilovsky, D. 1994. S_1 destabilazation and
566 higher sensitivity to light in metribuzin-resistant mutants. *Plant Physiol.* 104:235-45
567 Sarthou, G., Timmermans, K. R., Blain, S. & Tréguer, P. 2005. Growth physiology and
568 fate of diatoms in the ocean: a review. *J. Sea Res.* 53:25-41
569 Srivasatava, A., Mohanty, P. & Bose, S. 1994. Alterations in the excitation energy
570 distribution in *Synechococcus* PCC 7942 due to prolonged partial inhibition of

photosystem II. Comparison between inhibition caused by (a) presence of PSII inhibitors, (b) mutation in the D1 polypeptide of PSII. *Biochim. Biophys. Acta* 1186:1-11

van Rensen, J. J. S., Xu, C. & Govindjee 1999. Role of bicarbonate in photosystem II, the water-plastoquinone oxido-reductase of plant photosynthesis. *Physiol. Plant.* 105:585-92

Vass, I., Styring, S., Hundal, T., Koivuniemi, A., Aro, E.-M. & Andersson, B. 1992. Reversible and irreversible intermediates during photohinibition of photosystem II: Stable reduced Q_A species promote chlorophyll triplet formation. *Proc. Natl. Acad. Sci. USA* 89:1408-12

Vermaas, W., Vass, I., Eggers, B. & Styring, S. 1994. Mutation of a putative ligand to the non-heme iron in Photosystem II: Implications for Q(A) reactivity, electron transfer, and herbicide binding. *Biochim. Biophys. Acta* 1184:263-72

Wagner, H., Jakob, T. & Wilhelm, C. 2006. Balancing the energy flow from captured light to biomass under fluctuating light conditions. New Phytol. 169:95-108

Wilhelm, C., Büchel, C., Fisahn, J., Goss, R., Jakob, T., LaRoche, J., Lavaud, J., Lohr, M., Riebesell, U., Stehfest, K. & Kroth, P. 2006. The regulation of carbon and nutrient assimilation in diatoms is significantly different from green algae. *Protist* 157:91-124

Xiong, J., Hutchison, R. S., Sayre, R. T. & Govindjee 1997. Modification of the photosystem II acceptor side function in a D1 mutant (arginine-269-glycine) of *Chlamydomonas reinhardtii*. *Biochim. Biophys. Acta* 1322:60-76

Legends

Fig. 1: Western-blot of the D1 protein of the PSII reaction center of *P. tricornutum* wild-type (WT) and the *psbA* mutant L275W cells. Cells were grown at 50 µmol photons m^{-2} s^{-1}. Bands representing D1 degradation products of 23 kDa and the cross-link products of around 83 kDa also resulting from D1 degradation (Ishikawa et al. 1999) were found in a larger amount in L275W but not in the WT.

Fig. 2: A-Thermoluminescence emission of dark-adapted cells of *P. tricornutum* wild-type (WT) and the *psbA* mutants V219I / F255I / S264A. The characteristic emission bands at 7°C (Q) and 22°C (B) are shown; they reflect the recombination states of the PSII reaction center $S_2Q_A^-$ and $S_{2/3}Q_B^-$ and the redox potential of Q_A and Q_B, respectively (Gilbert et al. 2004; Eisenstadt et al. 2008). Curves are average of three measurements. B-O_2 production in a series of single-turnover flashes (O_2 sequences) by dark-adapted cells of *P. tricornutum* wild-type (WT) and of the two *psbA* mutants S264A and L275W, as measured via a flash electrode. The pattern of the O_2 sequence for V219I resembled the one of the WT, and the pattern of F255I resembled the one of S264A with less pronounced features. See Fig. S4 for a detailed description. C-/D-Chl *a* fluorescence induction kinetics reflect quantum yield changes of Chl *a* fluorescence as a function of the illumination duration, which relates to both excitation trapping in PSII and the ensuing photosynthetic electron transport; C- Short-time kinetics recorded via PEA fluorometer from dark-adapted cells of *P. tricornutum* wild-type (WT) and the four *psbA* V219I / F255I / S264A / L275W mutants. The letters O, J, I P, H, G refer to the phases of

613 the kinetics (Lazar 2006); D- Long-time kinetics from dark-adapted cells of WT and
614 L275W (same pattern for S264A) as recorded with a self-made 'continuous light'
615 fluorometer. The arrow indicates the first peak (I phase at 45 ms) which amplitude
616 reflects the redox state of Q_A (Lavaud and Kroth 2006). In diatoms, the classic P peak is
617 divided into two peaks H and G (Lazar 2006, Lavaud and Kroth, 2006).
618
619 Fig. 3: Chl *a* fluorescence parameters as recorded with a PAM-fluorometer for the wild-
620 type (WT) and the four *psbA* V219I / F255I / S264A / L275W mutants of *P. tricornutum*
621 cells as a function of a light intensity gradient from darkness (0 µmol photons m^{-2} s^{-1}) to
622 the equivalent of full sunlight in nature (2000 µmol photons m^{-2} s^{-1}, Long et al. 1994).
623 The illumination duration was 5 min; a new sample was used for each irradiance
624 treatment. A- 1-qP estimates the fraction of reduced Q_A (Büchel and Wilhelm 1993).
625 Inset: Ratio mutants *vs* WT of the amplitude of the I-45 ms peak (see Fig. 2D) up to 100
626 µmol photons m^{-2} s^{-1}. B- ETR is the rate of linear electron transport. See the materials and
627 methods section and Fig. S4 for details about the calculations of these parameters. Values
628 are average ± SD of three to four measurements.
629
630 Fig. 4: Diagram of the influence of mutations on the photosynthetic apparatus of the *psbA*
631 V219I / F255I / S264A / L275W mutants of *P. tricornutum* in comparison to the WT
632 situation. Left: the electron pathways within the PSII reaction center, right: the
633 architecture of the photosystems as a function of WT situation (PSI:PSII 1:2), arrow up,
634 increased value (the true value is given in-between brackets); arrow down, decrease; flat
635 arrow, no change. Symbols: red star, mutation; size of Q_A^-/Q_B^-, concentration of Q_A^-/Q_B^-;

636 thickness of the e^- arrows, value of the ETR_{max} and of the Q_B^- to Q_A back-transfer; dotted
637 feature of the OEC arrow, proportion of the disturbance of the OEC operation.
638 Abbreviations: E_K, light intensity for saturation of photosynthesis; e^-, electrons; LHC,
639 light-harvesting antenna complex; OEC, oxygen evolving complex; PSII/PS I RC,
640 photosystem I/photosystem II reaction center; PSI:PSII, molar photosystem
641 stoichiometry; Q_A and Q_B, quinones. See the text for a more detailed description.
642
643

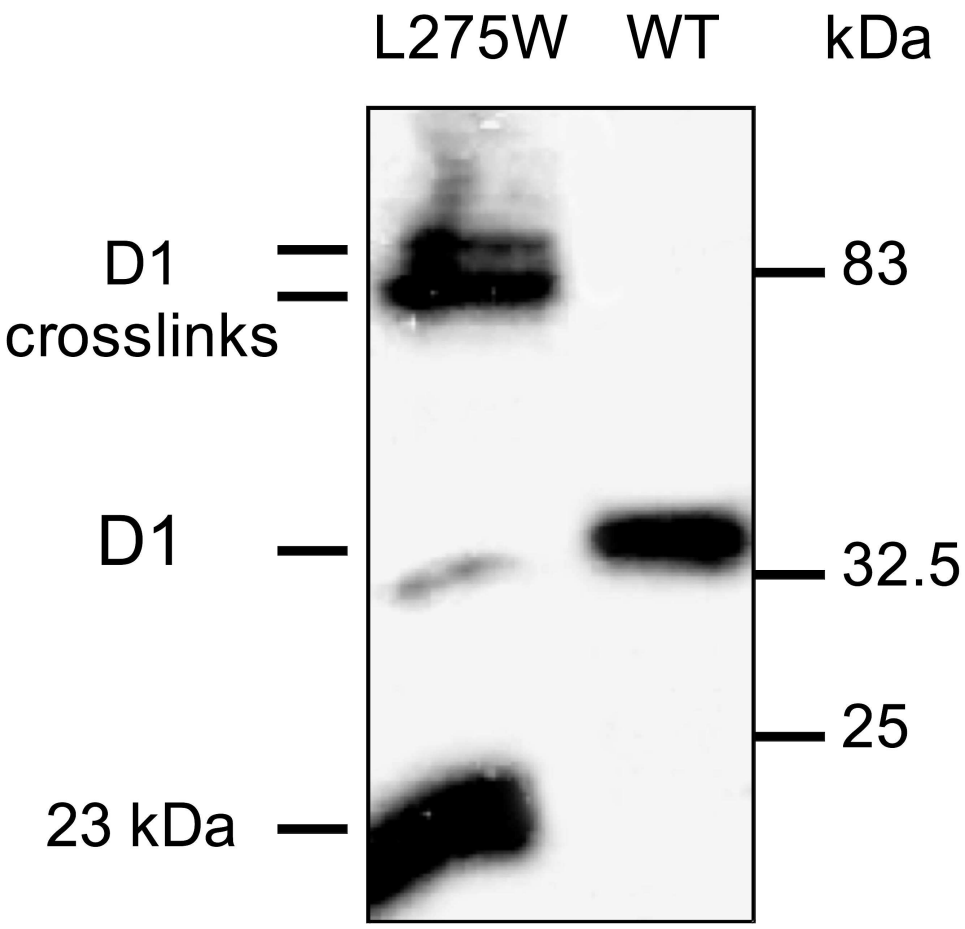

Figure 1
117x117mm (600 x 600 DPI)

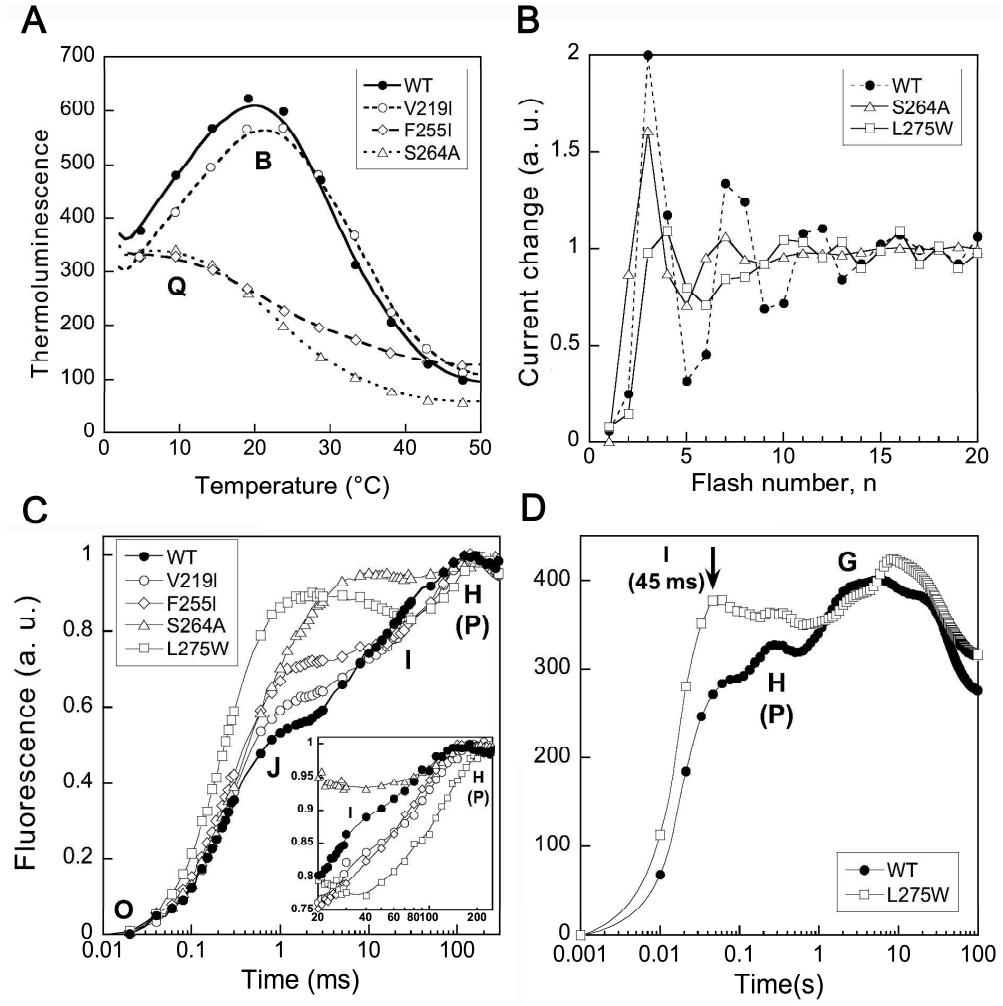
A
Thermoluminescence
Temperature (°C)
WT
V219I
F255I
S264A
B
Q
B
Current change (a. u.)
Flash number, n
WT
S264A
L275W
C
Fluorescence (a. u.)
Time (ms)
WT
V219I
F255I
S264A
L275W
O
J
I
H
(P)
D
I
(45 ms)
G
H
(P)
Time(s)
WT
L275W

Figure 2

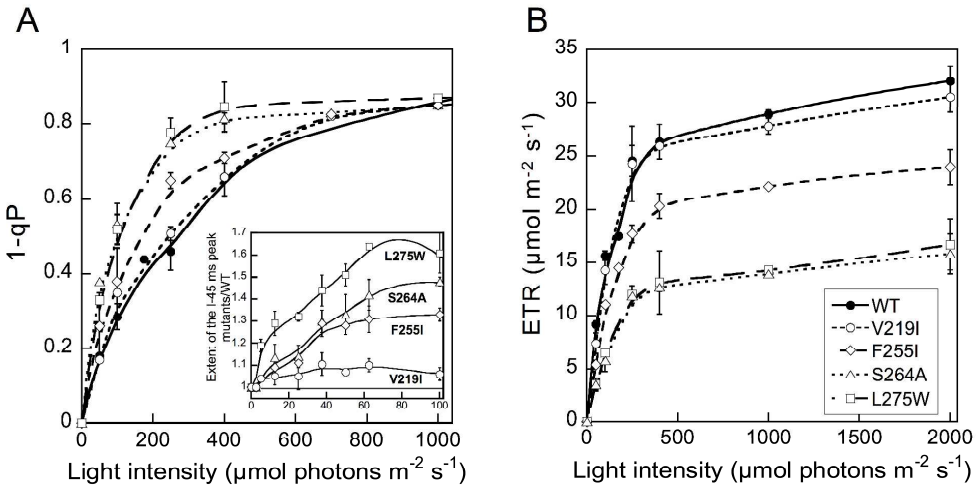

Figure 3
249x126mm (600 x 600 DPI)

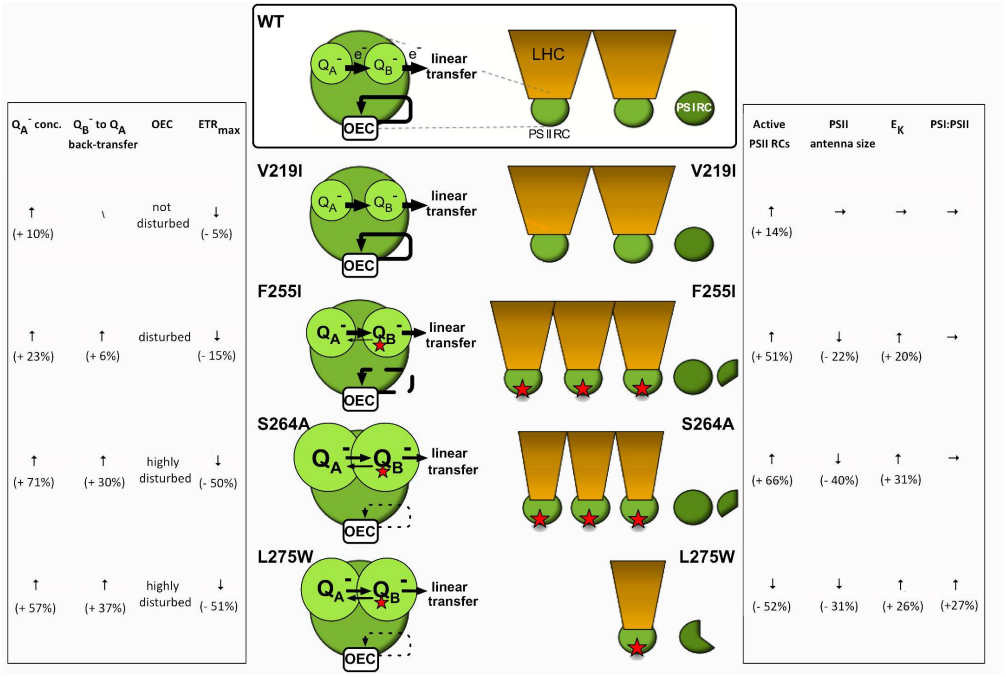

Figure 4

Supplementary File S1

Construction of the pGEM-T D1 transformation vectors

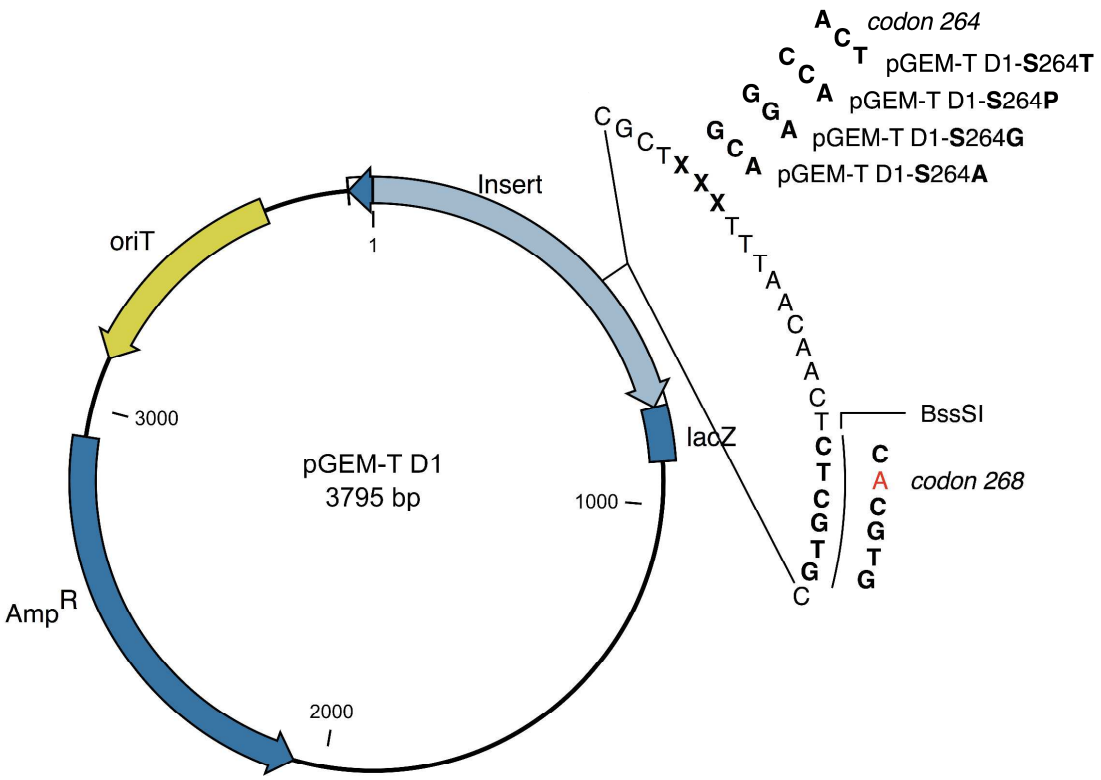

Using the primers P-psbA196-5' (5'-CTGTTGCAGGTTCTTTATTATATGG-3') and P-psbA990-3' (5'-TACTTCCATACCTAAATCAGCACGG-3') a 795 bp fragment of the plastid encoded *Phaeodactylum tricornutum* gene *psbA* was amplified following standard PCR procedures (Sambrook et al. 1995) and subsequently ligated into the insertion site of the commercially available TA cloning vector pGEM-T according to the manufacturer's instructions (Promega Corporation, Madison, WI, USA).

The resulting vector pGEM-T D1 was subject to site directed mutagenesis substituting the codon 264 (Ser) with four alternative codons that encode the amino acids Ala

(pGEM-T D1-S264A), Gly (pGEM-T D1-S264G), Pro (pGEM-T D1-S264P), and Thr (pGEM-T D1-S264T). Moreover, a *BssS*I recognition site was altered by a silent T to A nucleotide substitution in codon 268 (not altering the encoded amino acid sequence). Site directed mutagenesis was performed via round circle PCR using he primers D1-792-fw (5'-CGTTTAATCTTCCAATACGCTXXXTTTAACAACTCaCGTGC-3') and D1-792-rev (5'- GCACGTGAGTTGTTAAAXXXAGCGTATTGGAAGATTAAACG-3') and the pGEM-T D1 vectors as template. The XXX within the primer sequence refers to the altered codon (compared to the wild-type (WT) sequence) leading to the desired amino acid substitution. The small letter a in the D1-792-fw sequence indicates the second, conservative point mutation. Turbo-Pfu Polymerase (Stratagene, La Jolla, USA) was used for the round circle PCR reaction. The resulting products were treated with *Dpn*I for selective degradation of all non-modified (hence methylated) parent strands and subsequently transformed into chemically competent *E. coli* XL-1. The four resulting constructs served as transformation vectors in our attempts to transform the plastid genome of the diatom.

Supplementary File S2

Multiple sequence alignments and phylogenetic reconstruction

The strong selection pressure acting on *psbA* led to a high degree of sequence conservation that allows reconstructing a phylogeny of photosynthetic organisms based on the PsbA (D1) sequence that agrees well with more sophisticated phylogenetic reconstructions using more than one molecular marker (Delwiche 1999, Rodriguez-Ezpeleta et al. 2005).

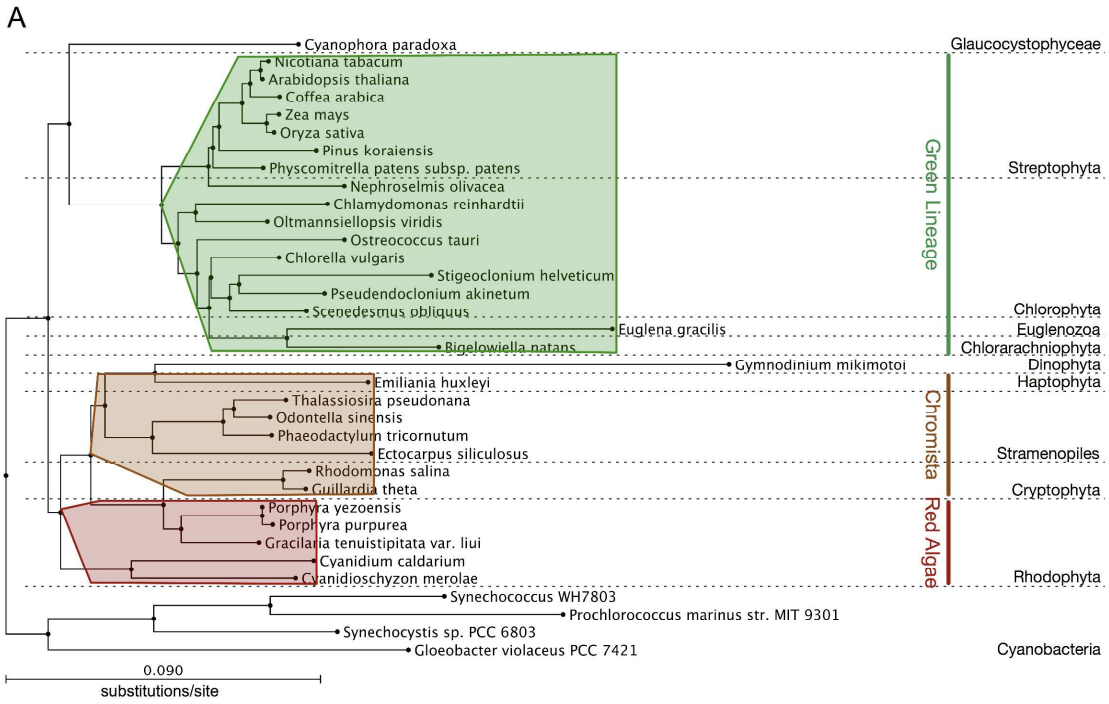

A- Phylogenetic tree (neighbor joining, 100 fold bootstrapping) of D1 (PsbA) reconstructed from the amino acid sequence alignment (MUSCLE algorithm (Edgar 2004) of 35 individual protein sequences (see below for complete list). Although reflecting the current knowledge on plastid evolution in photosynthetic eukaryotes the purpose of this phylogenetic reconstruction is not to draw evolutionary conclusions (few branches have bootstrap support of less than 50), but rather intends to highlight the conservation level of D1 and to list the species included in our analysis of the sequence conservation of the Q_B binding pocket. Three groups consisting of green algae, red algae, and glaucophytes directly derive from the primary endocytobiosis between a cyanobacterium and a eukaryotic heterotrophic cell. Euglenozoans and chlorarachniophytes are derived from secondary endocytobiosis between a green alga and a eukaryotic host cell. Secondary endocytobiotic engulfment of a red alga by a eukaryotic host gave rise to the heterokonts (or stramenopiles), cryptophytes, haptophytes and dinoflagellates (Delwiche 1999, Cavalier-Smith 2000).

B- Sequence alignment of the Q_B pocket within the D1 protein. Light grey boxes, D, DE and E helices; dark grey bars, His_{215} and His_{272} which bind a non-heme iron atom; red squares, localization of the point mutations (from left to right) V219I / F255I / S264A / L275W in *Phaeodactylum tricornutum psbA* mutants; light green boxes, amino acid substitutions to be transferred by the respective transformation vector. The conservation plot below the alignment shows the degree of conservation (in %) for every individual site. The blot was inferred from an amino acid sequence alignment of D1 proteins from the 35 species listed in the phylogenetic tree above (Fig S2A, or see complete list below). Synechocystis, *Synechocystis* sp. PCC6803 (cyanobacteria, NC_000911);

Synechococcus WH7803 (cyanobacteria, CT971583); C. reinhardtii, *Chlamydomonas reinhardtii* (Chlorophytes, AF396929); A. thaliana, *Arabidospsis thaliana* (Embryophytes, CAB10554), C. merolae, *Cyanidioschyzon merolae* 10D (Rhodophytes, BAC76132); T. pseudonana, *Thalassiosira pseudonana* (Heterokontophytes, Bacillariophyceae, EF067921); O. sinensis, *Odontella sinensis* (Heterokontophytes, Bacillariophyceae, CAA91657); P. tricornutum, *Phaeodactylum tricornutum* (Heterokontophytes, Bacillariophyceae, AY864816).

Methods:

All bioinformatic operations were performed using tools provided by the bioinformatic software package CLC Combined Workbench, Version 3.6.1 (CLC bio, Aarhus, Denmark). The phylogenetic tree for the D1 (PsbA) protein was reconstructed from an amino acid sequence alignment of entire D1 protein sequences from 35 different species (Fig. S3). For the alignment of protein sequences the MUSCLE algorithm was used (standard settings, maximal 16 iterations). The neighbor joining tree was reconstructed from the resulting alignment (data not shown), the value for the number of bootstrap replicates was set to 100. The tree was rooted above the common ancestor of the cyanobacteria. From the same alignment a conservation blot was inferred. Therefore the graphical alignment settings of the CLC Combined Workbench were set to 'Line plot'. For Fig S2B, amino acid sequences of the quinone B (Q_B) pocket (amino acid position 189 to 298) from eight species (Fig. S3) plus the translated sequencing results from the four mutant strains were aligned using the MUSCLE algorithm (standard settings, maximal 16 iterations).

References:

Cavalier-Smith, T. 2000. Membrane heredity and early chloroplast evolution. *Trends Plant Sci.* 5:174-82

Delwiche, C. F. 1999. Tracing the thread of plastid diversity through the tapestry of life. *Am. Nat.* 154:S164-77

Rodriguez-Ezpeleta, N., Brinkmann, H., Burey, S. C., Roure, B., Burger, G., Löffelhardt, W., Bohnert, H. J., Philippe, H., Lang, F. B. 2005. Monophyly of primary photosynthetic eukaryotes: Green plants, red algae and glaucophytes. Curr. Biol. 15:1325-1330

NCBI accession numbers of PsbA (D1) sequences (no particular order).

All listed *psbA* genes were used for the MUSCLE amino acid alignment of the entire protein sequence, from which the phylogenetic tree (Fig. S2A) was reconstructed. The conservation plot (Fig S4) has been derived from the same alignment.
A subset (*) of the *psbA* genes listed was used for the MUSCLE amino acid alignment of the Q_B pocket (Fig S2B). From another subset (†) the pairwise comparison of amino acid similarities and distances was inferred (Fig. S4).

ACCESSION CP000576
ORGANISM **Prochlorococcus marinus str. MIT 9301**
Bacteria; Cyanobacteria; Prochlorales; Prochlorococcaceae; Prochlorococcus.

ACCESSION NC_000911
ORGANISM **Synechocystis sp. PCC 6803*†**
Bacteria; Cyanobacteria; Chroococcales; Synechocystis.

ACCESSION CT971583
ORGANISM **Synechococcus sp. WH 7803*†**
Bacteria; Cyanobacteria; Chroococcales; Synechococcus.

ACCESSION BA000045
ORGANISM **Gloeobacter violaceus PCC 7421**
Bacteria; Cyanobacteria; Gloeobacteria; Gloeobacterales; Gloeobacter.

ACCESSION Z00044 S54304
ORGANISM **Nicotiana tabacum**
Eukaryota; Viridiplantae; Streptophyta; Embryophyta; Tracheophyta; Spermatophyta; Magnoliophyta; eudicotyledons; core eudicotyledons; asterids; lamiids; Solanales; Solanaceae; Nicotianoideae; Nicotianeae; Nicotiana.

ACCESSION X86563
ORGANISM **Zea mays**
Eukaryota; Viridiplantae; Streptophyta; Embryophyta; Tracheophyta;

ACCESSION EF044213
ORGANISM **Coffea arabica**
Eukaryota; Viridiplantae; Streptophyta; Embryophyta; Tracheophyta; Spermatophyta; Magnoliophyta; eudicotyledons; core eudicotyledons;

ACCESSION AY228468
ORGANISM **Pinus koraiensis**
Eukaryota; Viridiplantae; Streptophyta; Embryophyta; Tracheophyta; Spermatophyta; Coniferopsida; Coniferales; Pinaceae; Pinus; Strobus.

ACCESSION AY522329
ORGANISM **Oryza sativa** (indica cultivar-group)
Eukaryota; Viridiplantae; Streptophyta; Embryophyta; Tracheophyta; Spermatophyta; Magnoliophyta; Liliopsida; Poales; Poaceae; BEP

ACCESSION AP000423
ORGANISM **Arabidopsis thaliana***†
Eukaryota; Viridiplantae; Streptophyta; Embryophyta; Tracheophyta; Spermatophyta; Magnoliophyta; eudicotyledons; core eudicotyledons; rosids; eurosids II; Brassicales; Brassicaceae; Arabidopsis.

ACCESSION AB001684
ORGANISM **Chlorella vulgaris**†
Eukaryota; Viridiplantae; Chlorophyta; Trebouxiophyceae; Chlorellales; Chlorellaceae; Chlorella.

ACCESSION AF137379 L77928
ORGANISM **Nephroselmis olivacea**
Eukaryota; Viridiplantae; Chlorophyta; Prasinophyceae;

Pseudoscourfieldiales; Pycnococcaceae; Nephroselmis.

ACCESSION DQ291132
ORGANISM **Oltmannsiellopsis viridis**
Eukaryota; Viridiplantae; Chlorophyta; Oltmannsiellopsis.

ACCESSION AP006715
ORGANISM **Porphyra yezoensis**
Eukaryota; Rhodophyta; Bangiophyceae; Bangiales; Bangiaceae; Porphyra.

ACCESSION U38804
ORGANISM **Porphyra purpurea**†
Eukaryota; Rhodophyta; Bangiophyceae; Bangiales; Bangiaceae;

ACCESSION AY673996
ORGANISM **Gracilaria tenuistipitata var. liui**†
Eukaryota; Rhodophyta; Florideophyceae; Gracilariales; Gracilariaceae; Gracilaria.

ACCESSION AF022186 Z36235 Z70297
ORGANISM **Cyanidium caldarium**
Eukaryota; Rhodophyta; Bangiophyceae; Cyanidiales; Cyanidiaceae; Cyanidium.

ACCESSION AB002583
ORGANISM **Cyanidioschyzon merolae** strain 10D*†
Eukaryota; Rhodophyta; Bangiophyceae; Cyanidiales; Cyanidiaceae; Cyanidioschyzon.

ACCESSION EF067921
ORGANISM **Thalassiosira pseudonana***†
Eukaryota; stramenopiles; Bacillariophyta; Coscinodiscophyceae; Thalassiosirophycidae; Thalassiosirales; Thalassiosiraceae; Thalassiosira.

ACCESSION Z67753
ORGANISM **Odontella sinensi***†
Eukaryota; stramenopiles; Bacillariophyta; Coscinodiscophyceae; Biddulphiophycidae; Eupodiscales; Eupodiscaceae; Odontella.

ACCESSION U30821
ORGANISM **Cyanophora paradoxa**†
Eukaryota; Glaucocystophyceae; Cyanophoraceae; Cyanophora.

ACCESSION X70810

ORGANISM **Euglena gracilis**†
Eukaryota; Euglenozoa; Euglenida; Euglenales; Euglena.

ACCESSION AY741371
ORGANISM **Emiliania huxleyi**†
Eukaryota; Haptophyceae; Isochrysidales; Noelaerhabdaceae; Emiliania.

ACCESSION DQ630521 L49157
ORGANISM **Stigeoclonium helveticum**
Eukaryota; Viridiplantae; Chlorophyta; Chlorophyceae;

ACCESSION DQ396875 L43360
ORGANISM **Scenedesmus obliquus**
Eukaryota; Viridiplantae; Chlorophyta; Chlorophyceae; Sphaeropleales; Scenedesmaceae; Scenedesmus.

ACCESSION AY835431 L44125
ORGANISM **Pseudendoclonium akinetum**
Eukaryota; Viridiplantae; Chlorophyta; Ulvophyceae; Ulvales; Pseudendoclonium.

ACCESSION NC_008289
ORGANISM **Ostreococcus tauri**†
Eukaryota; Viridiplantae; Chlorophyta; Prasinophyceae; Mamiellales; Mamiellaceae; Ostreococcus.

ACCESSION BK000554 AF396929
ORGANISM **Chlamydomonas reinhardtii***
Eukaryota; Viridiplantae; Chlorophyta; Chlorophyceae; Chlamydomonadales; Chlamydomonadaceae; Chlamydomonas.

ACCESSION NC_005087
ORGANISM **Physcomitrella patens** subsp. patens
Eukaryota; Viridiplantae; Streptophyta; Embryophyta; Bryophyta; Moss Superclass V; Bryopsida; Funariidae; Funariales; Funariaceae; Physcomitrella.

ACCESSION AY864816
ORGANISM **Phaeodactylum tricornutum***†
Eukaryota; stramenopiles; Bacillariophyta; Bacillariophyceae; Bacillariophycidae; Naviculales; Phaeodactylaceae; Phaeodactylum.

ACCESSION DQ851108
ORGANISM **Bigelowiella natans**†
Eukaryota; Cercozoa; Chlorarachniophyceae; Bigelowiella.

ACCESSION EF508371
ORGANISM **Rhodomonas salina**
Eukaryota; Cryptophyta; Cryptomonadaceae; Rhodomonas.

ACCESSION AF041468 AF063017 M76547 U81044 X14171 X14504 X51511 X52158 X52912 X56806 X62348 X62349 Z21976
ORGANISM **Guillardia theta**†
Eukaryota; Cryptophyta; Cryptomonadaceae; Guillardia.

ACCESSION X56695
ORGANISM **Ectocarpus siliculosus**
Eukaryota; stramenopiles; Phaeophyceae; Ectocarpales; Ectocarpaceae; Ectocarpus.

ACCESSION AB027234 REGION: 4..1086
ORGANISM **Gymnodinium mikimotoi**†
Eukaryota; Alveolata; Dinophyceae; Gymnodiniales; Gymnodiniaceae; Gymnodinium.

Supplementary Figure S3

Pairwise comparison chart of D1 (PsbA) amino acid similarities and distances

		1	2	3	4	5	6	7	8	9	10	11	12	13	14	15	16	17	18
G. mikimotoi	1	100.00	88.18	85.45	88.18	86.36	84.55	86.36	86.36	86.36	84.55	84.55	87.27	86.36	84.55	86.36	85.45	86.36	88.18
E. huxleyi	2	0.13	100.00	92.73	95.45	93.64	95.45	91.82	94.55	90.91	91.82	90.91	93.64	94.55	92.73	92.73	92.73	92.73	94.55
T. pseudonana	3	0.16	0.08	100.00	97.27	97.27	92.73	90.00	90.91	91.82	92.73	89.09	91.82	92.73	92.73	90.91	92.73	91.82	90.91
O. sinensis	4	0.13	0.05	0.03	100.00	98.18	91.82	90.91	91.82	92.73	92.73	90.91	92.73	93.64	91.82	91.82	92.73	92.73	92.73
P. tricornutum	5	0.15	0.07	0.03	0.02	100.00	91.82	90.91	91.82	90.91	90.91	90.00	90.91	91.82	90.91	90.00	92.73	90.91	90.91
G. theta	6	0.17	0.05	0.08	0.09	0.09	100.00	93.64	94.55	90.00	90.00	90.00	93.64	94.55	93.64	91.82	93.64	90.91	90.91
P. purpurea	7	0.15	0.09	0.11	0.10	0.10	0.07	100.00	95.45	90.91	87.27	89.09	90.91	91.82	90.91	90.00	91.82	88.18	90.00
G. tenuistipitata var. liui	8	0.15	0.06	0.10	0.09	0.09	0.06	0.05	100.00	90.91	91.82	90.91	92.73	93.64	92.73	91.82	93.64	90.91	92.73
C. merolae	9	0.15	0.10	0.09	0.08	0.10	0.11	0.10	0.10	100.00	90.91	88.18	91.82	92.73	90.91	90.00	90.91	90.00	90.00
B. natans	10	0.17	0.09	0.08	0.08	0.10	0.11	0.14	0.09	0.10	100.00	90.00	94.55	94.55	93.64	94.55	91.82	92.73	92.73
E. gracilis	11	0.17	0.10	0.12	0.10	0.11	0.11	0.12	0.10	0.13	0.11	100.00	92.73	93.64	92.73	91.82	92.73	90.91	90.91
A. thaliana	12	0.14	0.07	0.09	0.08	0.10	0.07	0.10	0.08	0.09	0.06	0.08	100.00	99.09	96.36	98.18	95.45	93.64	91.82
C. vulgaris	13	0.15	0.06	0.08	0.07	0.09	0.06	0.09	0.07	0.08	0.06	0.07	0.01	100.00	97.27	97.27	96.36	94.55	92.73
O. tauri	14	0.17	0.08	0.08	0.09	0.10	0.07	0.10	0.08	0.10	0.07	0.08	0.04	0.03	100.00	95.45	96.36	92.73	91.82
C. reinhardtii	15	0.15	0.08	0.10	0.09	0.11	0.09	0.11	0.09	0.11	0.06	0.09	0.02	0.03	0.05	100.00	95.45	91.82	92.73
C. paradoxa	16	0.16	0.08	0.08	0.08	0.08	0.07	0.09	0.07	0.10	0.09	0.08	0.05	0.04	0.04	0.05	100.00	91.82	90.91
Synechococcus sp.	17	0.15	0.08	0.09	0.08	0.10	0.10	0.13	0.10	0.11	0.08	0.10	0.07	0.06	0.08	0.09	0.09	100.00	95.45
Synechocystis sp.	18	0.13	0.06	0.10	0.08	0.10	0.10	0.11	0.08	0.11	0.08	0.10	0.09	0.08	0.09	0.08	0.10	0.05	100.00

From a MUSCLE amino acid sequence alignment of a set of PsbA proteins (also see S3) a pairwise comparison of amino acid similarities and distances was inferred. The similarities are shown in % within and above the fields forming the diagonal from top left to bottom right of the chart. The values below the diagonal represent the Jukes-Cantor distances (corrected for multiple substitutions) between the two compared sequences (Jukes and Cantor, 1969). Red background indicates the highest values, blue background indicates the lowest values of the comparison. Highlighted by a black frame are the D1 similarities of all listed species with the three diatoms.

Methods:

All bioinformatic operations were performed using tools provided by the bioinformatic software package CLC Combined Workbench, Version 3.6.1 (CLC bio, Aarhus, Denmark). The pairwise comparison of amino acid sequence similarities/distances for the Q_B pocket was inferred from a MUSCLE alignment (standard settings, maximal 16

iterations, alignment not shown) of the Q_B pocket sequences (amino acid position 198 to 307) from 18 different species (see Fig. S2).

References:

Jukes, T. and Cantor, C. (1969). Mammalian Protein Metabolism, chapter Evolution of protein molecules, pages 21-32. New York: Academic Press.

Supplementary File S4

Pigment composition (in mol/100 mol chlorophyll *a* (Chl *a*)) and photosynthetic properties of the wild-type (WT) and the *psbA* mutants of *Phaeodactylum tricornutum*.

Pigment/Parameter	WT	V219I	F255I	S264A	L275W
DCMU resistance	/	3	150	3000	500
Chl *a* (pg cell^{-1})	0.50 ± 0.07	0.57 ± 0.08	0.53 ± 0.17	0.54 ± 0.03	0.57 ± 0.1
Diadinoxanthin	9.4 ± 2.1	8.2 ± 2.5	8.3 ± 0.4	8.4 ± 1.3	9.0 ± 2.1
Fucoxanthin	71.3 ± 5.7	74.3 ± 4.9	75.5 ± 2.8	69.4 ± 3.4	76.6 ± 4.0
Chl *c*	13.7 ± 0.7	14.7 ± 0.4	14.9 ± 1.3	14.2 ± 0.7	15.9 ± 1.7
β-carotene	7.7 ± 0.7	6.7 ± 1.0	6.6 ± 0.4	6.5 ± 1.3	6.0 ± 0.1
Y_{SS} (µg Chl a^{-1})	90 ± 11	103 ± 10	136 ± 7	149 ± 11	47 ± 4
RC/CS_0	158 ± 4	194 ± 4	216 ± 2	232 ± 1	n.d.
PSI:PSII	0.44 ± 0.04	0.46 ± 0.02	0.47 ± 0.03	0.43 ± 0.03	0.56 ± 0.07
$1/I_{1/2}$ of Y_{SS}	0.58	0.58	0.45	0.35	0.40
E_K (µmol photons m^{-2} s^{-1})	183 ± 5	189 ± 10	223 ± 20	240 ± 10	231 ± 10
J ($Q_AQ_B^-/Q_A^-Q_B^-$)	0.56 ± 0.06	0.61 ± 0.07	0.69 ± 0.09	0.96 ± 0.03*	0.88 ± 0.09
I ($Q_A^-Q_B^{2-}$)	0.89 ± 0.02	0.82 ± 0.03	0.82 ± 0.04	0.95 ± 0.02	0.81 ± 0.03
Misses/PSII	0.14 ± 0.01	0.14 ± 0.01	0.17 ± 0.01	0.23 ± 0.01	n.d.
F_0	131 ± 6	141 ± 11	139 ± 7.5	170 ± 9	180 ± 7
F_v/F_m	0.70 ± 0.02	0.68 ± 0.01	0.69 ± 0.01	0.71 ± 0.03	0.57 ± 0.01
Φ PSII	0.57 ± 0.06	0.56 ± 0.01	0.49 ± 0.02	0.39 ± 0.02	0.35 ± 0.04
ET_0/CS_0	182 ± 17	167 ± 4	145 ± 25	89 ± 17	75 ± 28
µ (d^{-1})	2.54 ± 0.2	2.72 ± 0.2	2.44 ± 0.3	2.38 ± 0.2	1.87 ± 0.1

Y_{SS} is the concentration of active PSII reaction centers per Chl *a* (Lavaud et al. 2002a); RC/CS_0 is the number of active PSII reaction center per PSII cross-section; $1/I_{1/2}$ of Y_{SS} is a measurement of the PSII light-harvesting antenna size (Lavaud et al. 2002a); E_K is the light intensity for saturation of photosynthesis; the DCMU resistance factor was calculated from the IC_{50} PSII fluorescence reactivity to DCMU; J (* J phase is delayed to 9.7 ± 2.5 ms in S264A) and I are the fluorescence levels of the J and I phases measured at 2 ms and 30 ms, respectively (values normalized to the P peak = 1, see Fig. 4A, P corresponds to the concentration of $Q_A^-Q_B^{2-}$ and PQH_2); F_0 is the minimal level of fluorescence of dark-adapted cells; F_v/F_m is the maximum photosynthetic efficiency of PSII, Φ PSII ($(F_m'-F')/F_m'$) is the effective PSII quantum yield for photochemistry measured at 50-100 µmol photons m^{-2} s^{-1} (an irradiance for which there is no NPQ); ET_0/CS_0 is the steady-state electron transport in a PSII cross-section; µ is the growth rate. All measurements were performed on cells grown at 50 µmol photons m^{-2} s^{-1}, which was low enough to prevent the de-epoxidation of diadinoxanthin into diatoxanthin. n. d., not determined. Values are average ± SD of three to four measurements. See the text for other details.

Methods:

DCMU resistance was evaluated measuring the inhibition of the PSII activity *vs* increasing DCMU concentrations using a self-made fluorometer (Parésys et al. 2005). The measure of inhibition is the increase in the amplitude of the I-45 ms peak illustrating the accumulation of Q_A^- due to the electron Q_A-Q_B transfer being blocked by DCMU (see Fig. 4B). This way, the IC_{50}, the DCMU concentration at which the PSII activity is inhibited by 50% was measured and compared between WT and mutants to evaluate a resistance factor.

Standard fluorescence nomenclature was used. F_0 and F_m are defined as the minimum PSII fluorescence yield of dark-adapted cells and the maximum PSII fluorescence yield reached

in such cells during a saturating pulse of white light, respectively. The PSII quantum yield for photochemistry is the ratio F_v/F_m where F_v is the variable part of the fluorescence emission and is equal to F_m-F_0. The photochemical quenching was qP = $(F_m\text{-}F')/(F_m'\text{-}F_0')$, where F' is the steady-state level of fluorescence emission reached after few minutes of illumination. 1-qP is a parameter to estimate the fraction of reduced Q_A (Büchel and Wilhelm 1993, Niyogi et al. 1998). A classic OIJP analysis was also performed (Strasser et al. 1995, Force et al. 2003) allowing to extract the following data: time to reach the J phase ($Q_AQ_B^-/Q_A^-Q_B^-$ state), time to reach the I phase ($Q_A^-Q_B^{2-}$ state), and the parameters RC/CS_0 and ET_0/CS_0 (Force et al. 2003).

For the control measurement of the relative O_2 yield produced per flash during a sequence of single-turnover saturating flashes (O_2 sequences), cells were first dark-adapted for 20 min and then deposited on the electrode. The cells were allowed to settle on the electrode for 7 min in darkness before measurement. The steady-state O_2 yield per flash (Y_{SS}) was attained for the last four flashes of a sequence of 20 flashes when the classical four-step oscillations due to the S-state cycle of the PSII RC O_2-evolving complex (Kok et al. 1970); see Fig. 4 for a classic recording) were fully damped. The oscillation is damped after a few cycles to a constant steady-state yield, Y_{SS}, due to loss of synchrony caused mainly by a non-zero probability of 'misses' (reflecting the number of PSII RCs unable to perform a charge separation during a flash, Lavorel 1976). Y_{SS} was used to evaluate the number of O_2 producing PSII RCs relative to Chl *a* (see Lavaud et al. 2002). The miss probability per PS II was calculated from the Lavorel matrix (Lavorel 1976). For the saturation curves of Y_{SS}, the intensity of the flashes was varied with neutral density filters. A new dark-adapted sample was used for each flash intensity measurement. $1/I_{1/2}$ of Y_{SS}, the reciprocal of the half-saturating flash intensity of flash O_2 evolution saturation curves was used as a measure of the PSII antenna size (Lavaud et al. 2002).

E_K, the irradiance for saturation of photosynthetic O_2 emission was estimated from P/E curves.

References:

Büchel, C. & Wilhelm, C. 1993. *In vivo* analysis of slow chlorophyll fluorescence induction kinetics in algae: progress, problems and perspectives. *Photochem. Photobiol.* 58:137-48

Force, L., Critchley, C. & van Rensen, J. J. S. 2003. New fluorescence parameters for monitoring photosynthesis in plants. 1. The effect of illumination on the fluorescence parameters of the JIP-test. *Photosynth. Res.* 78:17-33

Kok, B., Forbush, B. & McGloin, M. 1970. Cooperation of charges in photosynthetic O_2 evolution-I. A linear four step mechanism. *Photochem. Photobiol.* 11:457-75

Lavaud, J., van Gorkom, H. & Etienne, A.-L. 2002. Photosystem II electron transfer cycle and chlororespiration in planktonic diatoms. *Photosynth. Res*. 74:51-59

Lavorel, J. 1976. Matrix analysis of the oxygen evolving system of photosynthesis. *J. Theor. Biol.* 57:171-85

Niyogi, K. K., Grossman, A. R. & Bjorkman, O. 1998. *Arabidopsis* mutants define a central role for the xanthophyll cycle in the regulation of photosynthetic energy conversion. *Plant Cell* 10:1121-34

Parésys, G., Rigart, C., Rousseau, B., Wong, A. W. M., Fan, F., Barbier, J.-P. & Lavaud, J. 2005. Quantitative and qualitative evaluation of phytoplankton populations by trichromatic chlorophyll fluorescence excitation with special focus on cyanobacteria. *Water Res.* 39:911-21

Strasser, R. J., Srivasatava, A. & Govindjee 1995. Polyphasic chlorophyll *a* fluorescence transient in plants and cyanobacteria. *Photochem. Photobiol.* 61:32-4

Supplementary File S5

Growth curves of the wild-type (WT) and the four *psbA* V219I / F255I / S264A / L275W mutants of *P. tricornutum* cells.

Growth curves were performed under a light regime of 50 µmol photons m^{-2} s^{-1}/16:8 h light:dark. The cells were sampled each day 3 h after initiating the light period. Values are average ± SD of three to four measurements.

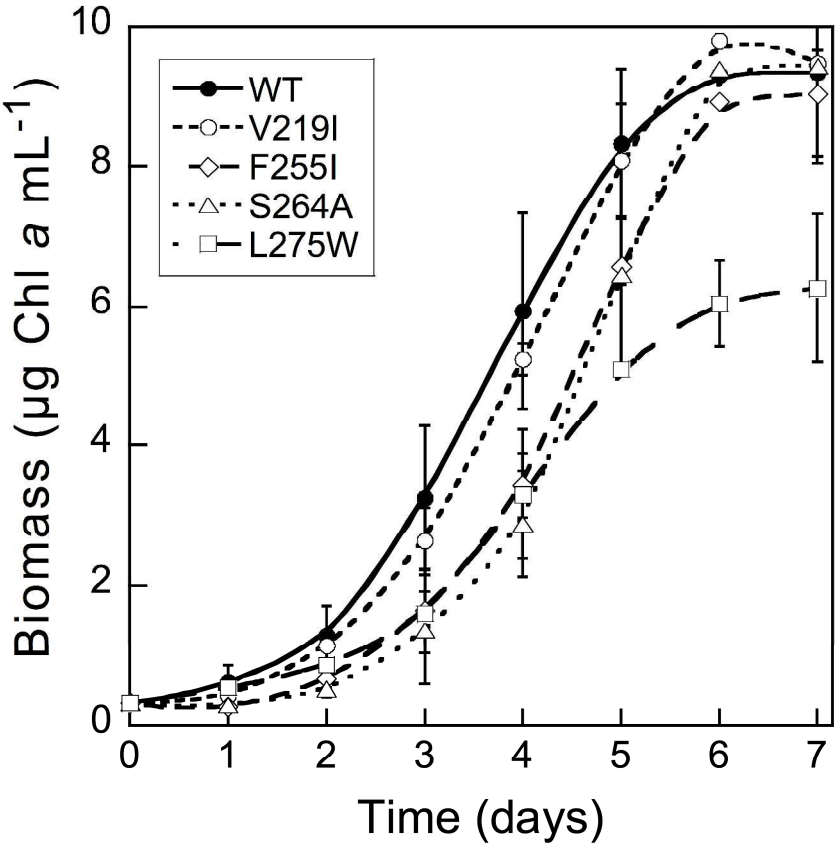

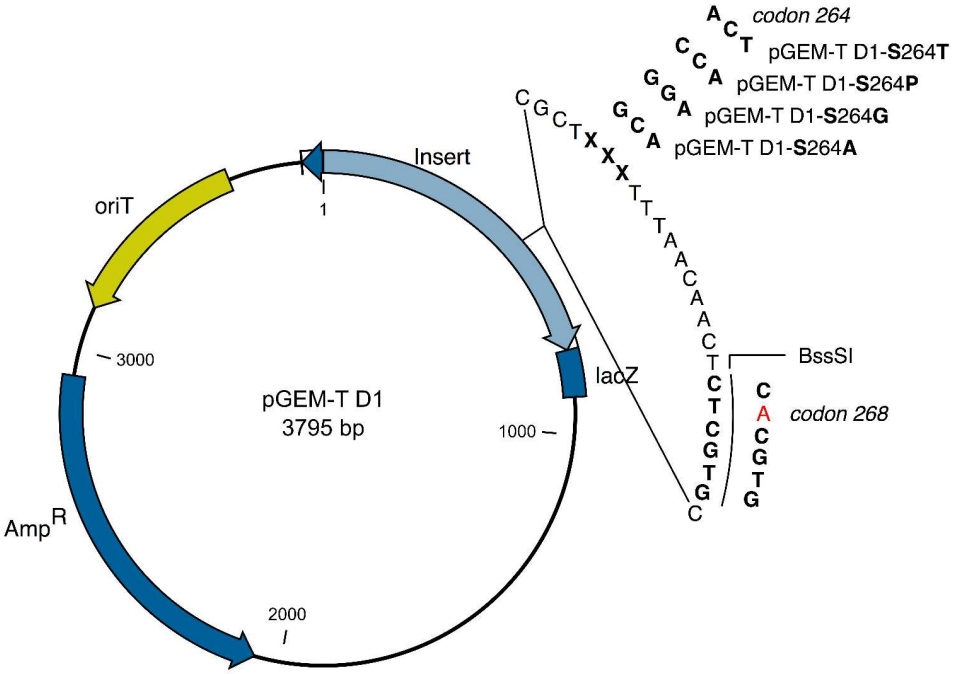

Figure S1
201x159mm (600 x 600 DPI)

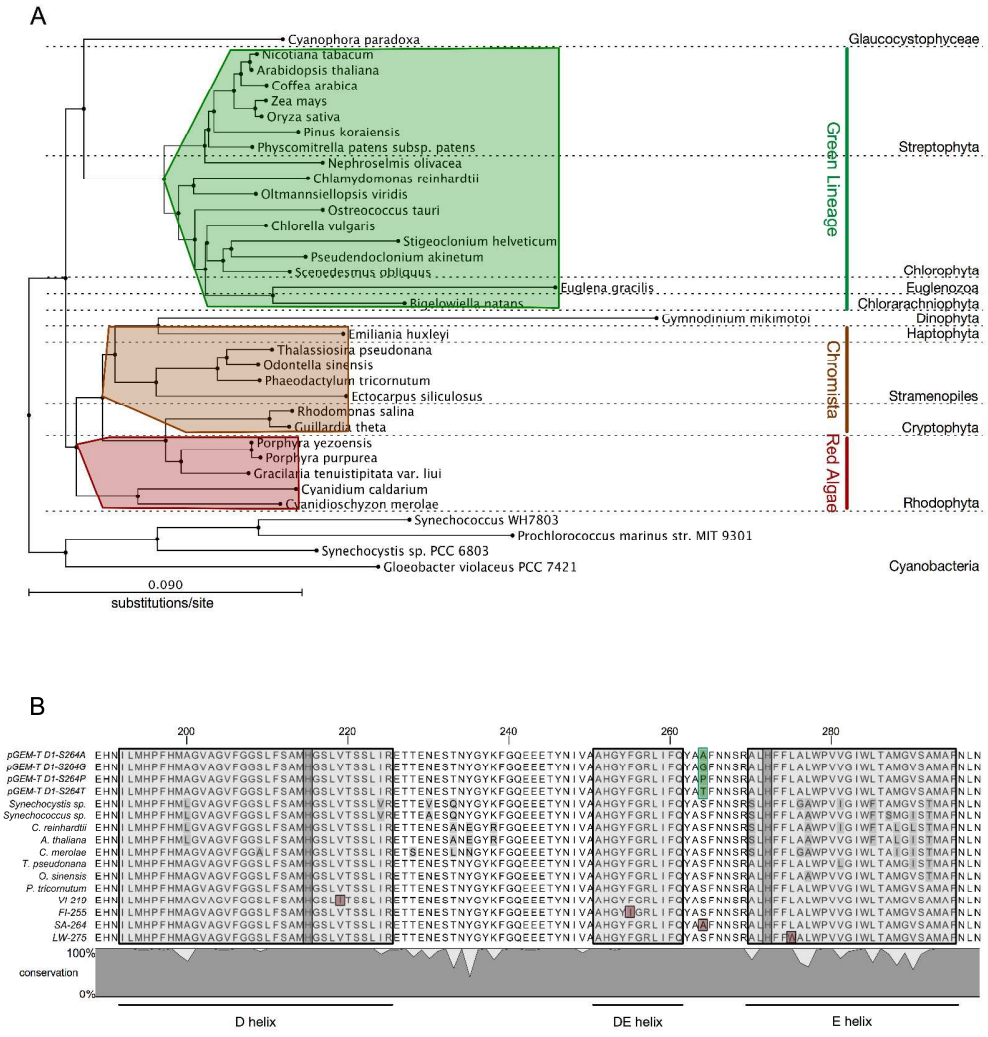

Figure S2
203x210mm (600 x 600 DPI)

		1	2	3	4	5	6	7	8	9	10	11	12	13	14	15	16	17	18
G. mikimotoi	1	100.00	88.18	85.45	88.18	86.36	84.55	86.36	86.36	86.36	84.55	84.55	87.27	86.36	84.55	86.36	85.45	86.36	88.18
E. huxleyi	2	0.13	100.00	92.73	95.45	93.64	95.45	91.82	94.55	90.91	91.82	90.91	93.64	94.55	92.73	92.73	92.73	92.73	94.55
T. pseudonana	3	0.16	0.08	100.00	97.27	97.27	92.73	90.00	90.91	91.82	92.73	89.09	91.82	92.73	92.73	90.91	92.73	91.82	90.91
O. sinensis	4	0.13	0.05	0.03	100.00	98.18	91.82	90.91	91.82	92.73	92.73	90.91	92.73	93.64	91.82	91.82	92.73	92.73	92.73
P. tricornutum	5	0.15	0.07	0.03	0.02	100.00	91.82	90.91	91.82	90.91	90.91	90.00	90.91	91.82	90.91	90.00	92.73	90.91	90.91
G. theta	6	0.17	0.05	0.08	0.09	0.09	100.00	93.64	94.55	90.00	90.00	90.00	93.64	94.55	93.64	91.82	93.64	90.91	90.91
P. purpurea	7	0.15	0.09	0.11	0.10	0.10	0.07	100.00	95.45	90.91	87.27	89.09	90.91	91.82	90.91	90.00	91.82	88.18	90.00
G. tenuistipitata var. liui	8	0.15	0.06	0.10	0.09	0.09	0.06	0.05	100.00	90.91	91.82	90.91	92.73	93.64	92.73	91.82	93.64	90.91	92.73
C. merolae	9	0.15	0.10	0.09	0.08	0.10	0.11	0.10	0.10	100.00	90.91	88.18	91.82	92.73	90.91	90.00	90.91	90.00	90.00
B. natans	10	0.17	0.09	0.08	0.08	0.10	0.11	0.14	0.09	0.10	100.00	90.00	94.55	94.55	93.64	94.55	91.82	92.73	92.73
E. gracilis	11	0.17	0.10	0.12	0.10	0.11	0.11	0.12	0.10	0.13	0.11	100.00	92.73	93.64	92.73	91.82	92.73	90.91	90.91
A. thaliana	12	0.14	0.07	0.09	0.08	0.10	0.07	0.10	0.08	0.09	0.06	0.08	100.00	99.09	96.36	98.18	95.45	93.64	91.82
C. vulgaris	13	0.15	0.06	0.08	0.07	0.09	0.06	0.09	0.07	0.08	0.06	0.07	0.01	100.00	97.27	97.27	96.36	94.55	92.73
O. tauri	14	0.17	0.08	0.08	0.09	0.10	0.07	0.10	0.08	0.10	0.07	0.08	0.04	0.03	100.00	95.45	96.36	92.73	91.82
C. reinhardtii	15	0.15	0.08	0.10	0.09	0.11	0.09	0.11	0.09	0.11	0.06	0.09	0.02	0.03	0.05	100.00	95.45	91.82	92.73
C. paradoxa	16	0.16	0.08	0.08	0.08	0.08	0.07	0.09	0.07	0.10	0.09	0.08	0.05	0.04	0.04	0.05	100.00	91.82	90.91
Synechococcus sp.	17	0.15	0.08	0.09	0.08	0.10	0.10	0.13	0.10	0.11	0.08	0.10	0.07	0.06	0.08	0.09	0.09	100.00	95.45
Synechocystis sp.	18	0.13	0.06	0.10	0.08	0.10	0.10	0.11	0.08	0.11	0.08	0.10	0.09	0.08	0.09	0.08	0.10	0.05	100.00

Figure S3
207x78mm (600 x 600 DPI)

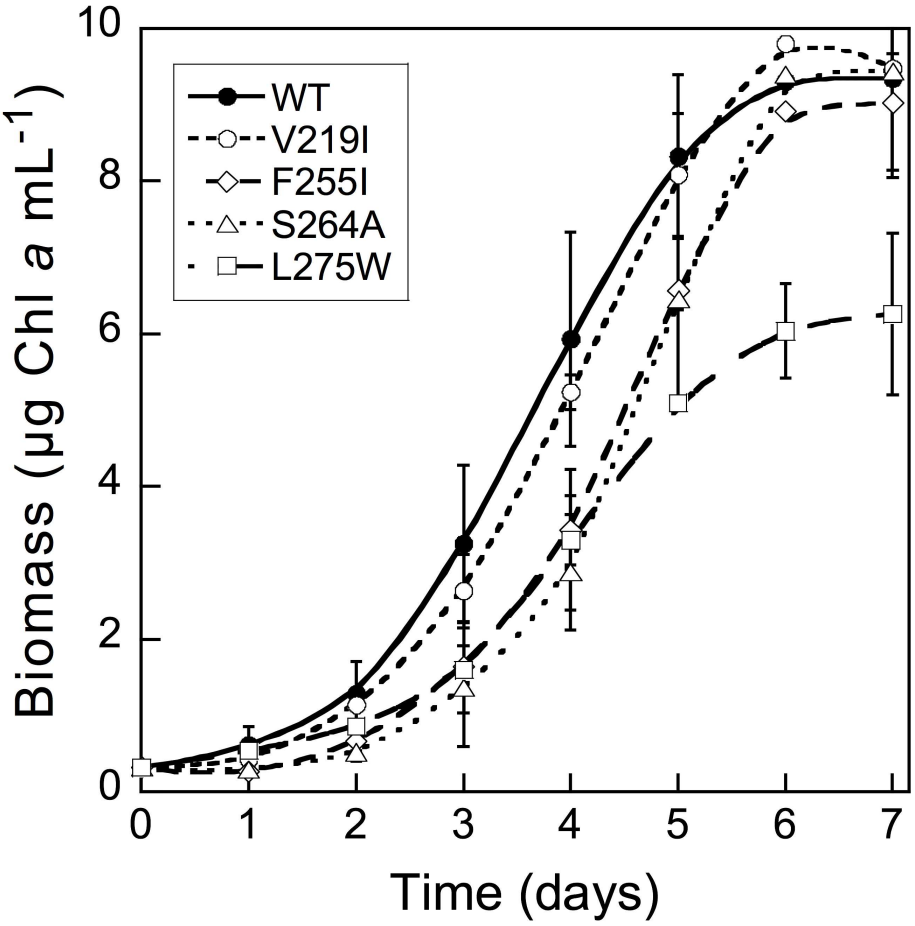

Figure S5
121x118mm (600 x 600 DPI)